CHALMERS

UNIVERSITY OF TECHNOLOGY

Evaluation of a Novel Concept
for Combined $\mathrm{NO_x}$ and $\mathrm{SO_x}$ Removal

Master's thesis in Master Programme Sustainable Energy Systems

JÜRGEN HAUNSTETTER
NIKO WEINHART

Evaluation of a Novel Concept for Combined NO$_x$ and SO$_x$ Removal

Jürgen Haunstetter
Niko Weinhart

Evaluation of a Novel Concept
for Combined NO$_x$ and SO$_x$ Removal
Jürgen Haunstetter
Niko Weinhart

Cover: Flowsheet of the new NO$_x$ and SO$_x$ removal concept constructed in ASPEN PLUS.

Evaluation of a Novel Concept
for Combined NO$_x$ and SO$_x$ Removal
Jürgen Haunstetter
Niko Weinhart
Department of Energy and Environment
Division of Energy technology
Chalmers University of Technology

Abstract

NO$_x$ and SO$_x$ are major air pollutants. Although there are already several flue gas cleaning methods on the market, research to find more effective and cost efficient measures is necessary. Most of the common measures use reduction for NO$_x$ removal and treat NO$_x$ and SO$_x$ separately. The present work describes a new NO$_x$ and SO$_x$ removal concept based on oxidation that treats both, simultaneously. Therefore the two main components of the concept, a reactor and an absorber, were modelled with ASPEN PLUS. The reactor, also called oxidizer uses chlorine dioxide as an oxidation agent. For the scrubbing solution in the absorber pure water, nitrous acid and pH control were tested.

The reactor simulation model was validated by experimental results of an appropriate test rig. Then the effects on the absorption of different flue gas and absorbent conditions were tested. Afterwards, further process conditions were tested on the complete removal concept.

The reactor model shows that the tested residence time and temperature has no effect on the NO conversion, whereas higher residence time increases and higher temperature decreases SO$_2$ conversion in the reactor. The outcome of the scrubber model is that Cl compounds as well as nitrogen oxides get sufficiently absorbed, whereas SO$_2$ cannot be sufficiently removed with reasonable water amounts. By using pH control and HNO$_2$ a positive effect on SO$_x$ removal was achievable.

Keywords: flue gas cleaning, NO oxidation, NO$_x$ and SO$_x$ kinetics, process simulation.

Acknowledgements

Contents

List of Figures

List of Tables

Abbreviations and Symbols

Symbols

C	Concentration	kmole s^{-1}
D	Pollutant diffusivity	m^2 s^{-1}
E	Activation Energy	J mole^{-1}
F	Mass flux	kmole m^{-2} s^{-1}
K_{eq}	Equilibrium constant	kmole m^{-3}
K_H	Henry's volatile constant	-
k	Pre-exponential factor	m^3 kmole^{-1} s^{-1}
n	Temperature exponent	-
R	Gas law constant	J K^{-1} mole^{-1}
r	Rate of reaction	kmole m^{-3} s^{-1}
T	Temperature	K
T_0	Reference temperature	K
v_{tot}	Total velocity	m s^{-1}
z	Layer thickness	mm

Subscripts

l	Liquid
g	Gas

Abbreviations

MFC	Mass flow controller
RCSTR	Rigorous continuous stirred tank reactor
REquil	Equilibrium reactor
L/G-ratio	Liquid to gas ratio

Abbreviations of chemical compounds

Cl$^-$	Chloride		NH$_4$NO$_3$	Ammonium nitrate
Cl$_2$	Chlorine		NO	Nitrogen monoxide
ClO	Chlorine monoxide		NO$_2$	Nitrogen dioxide

ClO_2	Chlorine dioxide		NO_2^-	Nitrite ion
CO_2	Carbon dioxide		NO_3^-	Nitrate
H^+	Hydron (positive hydrogen ion)		N_2O_3	Dinitrogen trioxide
HADS	Hydroxylamine disulfonic acid		N_2O_4	Dinitrogen tetroxide
HCl	hydrochloric acid		N_2O_5	Dinitrogen pentoxide
HNO	Nitroxyl		NO_x	Term for nitrogen oxides
HNO_2	Nitrous acid		O_3	Ozone
HNO_3	Nitric acid		S	Sulfur
H_2O	Water		SO_2	Sulfur dioxide
H_2SO_3	Sulfurous acid		SO_3	Sulfur trioxide
H_2SO_4	Sulfuric acid		SO_3^{2-}	Sulfite
N	Nitrogen		SO_4^{2-}	Sulfate
NH_3	Ammonia		SO_x	Term for sulfur oxides
NH_4NO_2	Ammonium nitrite			

1

Introduction

This thesis evaluates a new concept for the removal of nitrogen oxides and sulfur oxides from flue gases. Nitrogen oxides (NO_x) and sulfur oxides (SO_x) are major air pollutants, formed mainly during combustion processes. Those air pollutants cause acid rain, photochemical smog as well as ozone accumulation and adverse effects on human health. Therefore strict emission limitation standards exists in the developed part of the world. For example the limits set by the European Union are listed in Table 1.1.

Table 1.1: European Union emission limits for power plants for NO_x and SO_x in mg Nm^{-3} [36].

Plant Size	Coal		Biomass		Oil		Gas	
MW	NO_x	SO_x	NO_x	SO_x	NO_x	SO_x	NO_x	SO_x
100 − 300	200	200	200	200	150	200	100	35
> 300	150	150	150	150	100	150	100	35

To be able to apply to these limitations, flue gas treatment processes are required. SO_x emissions are mainly present as SO_2 in the flue gas and can be significantly reduced by different measures. The most common one is the wet scrubbing process. Here the SO_2 is washed out of the exhaust gas by using water and additives in so called scrubbing towers. This is possible due to the solubility of SO_2 which is 110 g L^{-1} at 20 °C.

The content of NO_x cannot be removed so easily. This is caused by the prevailing oxidation state of nitrogen, mainly $+2$, in the flue gas. This leads to the fact that most of the NO_x in the exhaust gas is formed to nitrogen monoxide (NO). This nitrogen compound is not soluble (0.056 g L^{-1} at 20 °C) and impossible to scrub. Consequently NO_x control is mostly achieved by reducing NO_x to N_2 with primary measures during combustion or chemical reduction techniques, such as selective catalytic reduction (SCR), downstream of the combustion process. These processes can achieve high reduction rates but are expensive.

The present work focus on a new concept, which consists of a two stage separation process, shown in Figure 1.1. The first part is based on the gas-phase oxidation of NO and SO_2, which takes part in a reactor, also called oxidizer. This oxidation is accomplished with chlorine dioxide (ClO_2) as an oxidizing agent to convert the rather insoluble NO to the more soluble NO_2 (29.2 g L^{-1} at 20 °C). Therefore this process enhances the removal of NO_x in wet scrubbers. The wet scrubber also called

absorber builds the second part of the system, where the pollutants are removed.
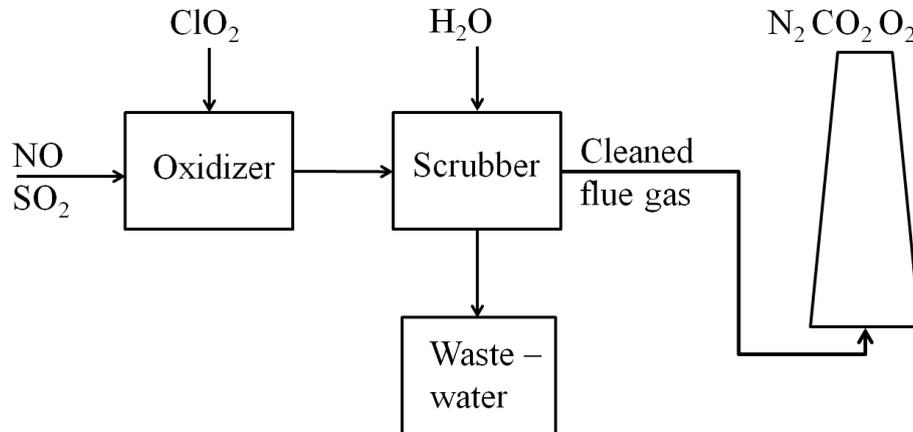
Figure 1.1: Simplified process diagram of the investigated removal concept with ClO_2.

Aim and structure of the work

The overall objective of the project is to evaluate the design of the ClO_2 process for NO_x and SO_x removal under conditions relevant to the flue gas output of power plants, by modeling. The aim may be divided into three parts:

- **Gas-phase:** Getting a better understanding of the different reactions happening in the gas-phase, between nitrogen, sulfur and chlorine compounds. For this purpose experiments with NO, SO_2 and ClO_2 are carried out by using the experimental facilities of AkzoNobel in Bohus.
  Afterwards transmission of the gained knowledge into the simulation model is done. For the modeling the simulation software ASPEN PLUS is used.

- **Liquid-phase:** The objective of this part is to model the absorber for the concept. Therefore the liquid-phase reactions have to be considered. This is based on the work by Ajdari et al. 2014. The model is tested by using different incoming conditions.

- **Complete design:** Finally both, the gas- and the liquid-phase model are merged to get the complete design of the new removal concept. The concept is then evaluated for the flue gas composition of a coal power plant. Furthermore the efficiency of NO_x and SO_x removal is considered.

The present study is structured in following chapters:

Motivation as well as the objectives are presented in chapter one.

In the second chapter NO_x formation mechanisms, state of the art removal measures as well as the chemistry for the gas- and liquid phase are constituted.

The third and fourth chapters deal with the methodology of the experiments as well as the simulations. Here the reactions of each phase are considered more precisely.

In the following fifth to seventh chapters the simulation performance of different flue gas conditions and inlet parameters are illustrated. Thereby a validation of the reactor model takes place. Afterwards the gained results are discussed.

Finally the conclusion and future prospects are explained in chapter eight and nine.

2

Theory

In this chapter the mechanisms of formation of nitrogen oxides in power plants are presented. Furthermore the state of the art nitrogen oxide removal options are introduced and typical advantages and disadvantages are discussed. The chemistry of NO_x and SO_x in both the gas- and liquid-phase are discussed.

2.1 NO_x-formation

There are three mechanisms for the formation of NO_x. These are classified as fuel, thermal and prompt NO_x. As shown in Figure 2.1 one of the main influencing parameter on NO_x formation is temperature. The other highly influencing parameter is the amount of nitrogen present in the fuel and the amount of nitrogen that is volatile bound. The fuel NO_x is formed through oxidization of fuel bound nitrogen, an example is given as Reaction 2.1. This mechanism is less temperature dependent than the other two and more dependent on the fuel to air ratio.

Thermal and prompt NO_x are both formed by oxidation of the nitrogen present in the combustion air. The thermal NO_x is generated in reaction with dissociated oxygen at high temperatures as shown in Reaction 2.2. Influencing parameters on thermal NO_x formation are the residence time, the oxygen level and, as mentioned before, the temperature in the reaction zone. Whereas prompt NO_x is formed due to fuel radicals at high peak point temperatures (compare reaction 2.3). Prompt NO_x is only significant in fuel rich zones and is also depending on the temperature [1, 11].

Fuel NO (example reaction):

$$NH_2 + \frac{1}{2}O_2 \longrightarrow NO + H_2 \tag{2.1}$$

Thermal NO (>1300 °C):
$$O + N_2 \longrightarrow NO + N \tag{2.2}$$
$$N + O_2 \longrightarrow NO + O$$
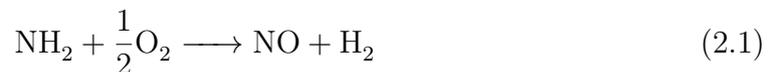
Prompt NO (>1500 °C):
$$CH + N_2 \longrightarrow HCN + N \tag{2.3}$$
$$HCNCN + O \longrightarrow NO + R$$
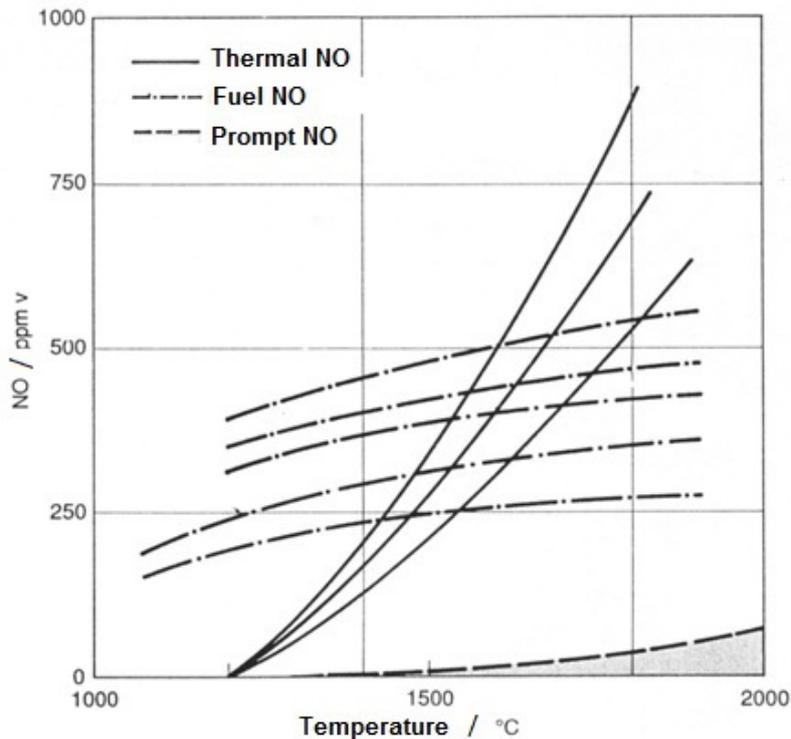
Figure 2.1: Dependency between NO formation mechanism and combustion temperature (lines form the region of each mechanism) [2].

2.2 NO_x removal measures

The reduction options are structured in two main categories. The so called primary measures reduces the generation of NO_x during the combustion. While the other category, the secondary measures, remove the nitrogen oxide afterwards from the flue gas stream.

2.2.1 Primary measures

The primary reduction options influence mainly the thermal NO_x, whereas prompt NO_x is of minor importance. These measures aim to modify not only the operational but also the design parameters of combustion installations in such a way, that nitrogen oxides already formed are converted inside the boiler or the formation of NO_x is reduced. The varied parameters are for example the temperature, the retention time at high temperatures, the oxygen in the reaction zone and the peak temperatures [11].
The mainly used primary options are air or fuel staging, slight preheating and flue gas recirculation. Air and fuel staging aim on low oxygen content and lower temperature in the reaction zone to reduce NO_x formation. Due to preheating also the combustion temperature rises, so for processes where preheating is not necessary for complete combustion, slight preheating is used to reduce the NO_x formation. Another way is the flue gas recirculation, here the NO_x formation is decreased in two ways. First the

cooled as well as relatively inert recirculated exhaust gas acts like a heat sink and therefore lowers the peak flame temperatures. The second way is that the average oxygen content of the combustion air is decreased and hence the NO_x formation [11].

2.2.2 Secondary measures

As secondary NO_x removal options simple scrubbing processes are not suitable. The reason for this is that the main NO_x component in the flue gas is nitrogen monoxide which dissolves not well in water. Therefore other processes have to be implemented. Those are using two different principles. On the one hand side the reduction of NO to molecular nitrogen and on the other hand the oxidation of NO by oxidation agents like ozone to the more soluble NO_2 or other higher soluble nitrogen oxide compounds.

Selective reduction processes

The selective reduction processes are divided into two measures. The first one is the selective non-catalytic reduction (SNCR), here high temperatures for the process are needed. By installing a catalyst the reaction activation energy can be reduced and thus the process temperature can be decreased. This measure is known as selective catalytic reduction (SCR).
Both reduce the NO_x to elementary nitrogen by adding a reducer agent, mostly ammonia. This happens downstream the furnace, but upstream the further flue gas treatments as precipitators for particulate matter and desulfurization plants (e.g. wet scrubbers). For achieving a good reduction rate, it is important that the reducing agent is injected in certain temperature intervals. If it is injected at too high temperatures it reacts with oxygen, generating more NO_x, whereas too low temperatures lead ammonia slip and a poor reduction efficiency [10].

SNCR: For the non-catalytic reduction three different reducing agents are commonly used, namely ammonia, urea and caustic ammonia. Each of them has a slightly different optimal temperature range. Important for achieving a good efficiency with the SNCR is a good mixing of the reducing agent with the NO_x and the injection within the temperature interval, which is quite narrow (overall: 900 °C – 1100 °C, for ammonia: 900 °C – 1000 °C). Within this optimal range efficiencies of up to 80% can be achieved. [10, 11].

Following reactions (2.4 and 2.5) take place by using ammonia as a reagent. If the temperatures exceed the temperature range, the second reaction 2.5 dominates, leading to an increase of NO_x and is therefore undesired [35].

$$4\,NO + 4\,NH_3 + O_2 \longrightarrow 4\,N_2 + 6\,H_2O \tag{2.4}$$

$$4\,NH_3 + 5\,O_2 \longrightarrow 4\,NO + 6\,H_2O \tag{2.5}$$
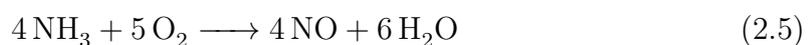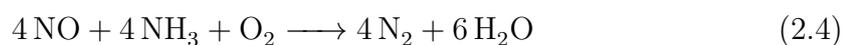
SCR: The SCR measure is based on the selective nitrogen oxide reduction with a reducing agent, while a catalyst is present. The reason for the useage of a catalyst is

to lower and widen the temperature range, as well as for improving the efficiency to $85\% - 90\%$. The temperature range is between $250\,°C - 500\,°C$ depending on the catalyst. As an reducing agent ammonia or urea is used, therefore different reactions can take place.[11]

1. Ammonia as a reducing agent:

$$4\,NO + 4\,NH_3 + O_2 \longleftrightarrow 4\,N_2 + 6\,H_2O \tag{2.6}$$

$$6\,NO_2 + 8\,NH_3 \longleftrightarrow 7\,N_2 + 12\,H_2O \tag{2.7}$$

2. Urea as a reducing agent:

$$4\,NO + 2\,(NH_2)_2CO + 2\,H_2O + O_2 \longleftrightarrow 4\,N_2 + 6\,H_2O + 2\,CO_2 \tag{2.8}$$

$$6\,NO_2 + 4\,(NH_2)_2CO + 4\,H_2O \longleftrightarrow 7\,N_2 + 12\,H_2O + 4\,CO_2 \tag{2.9}$$
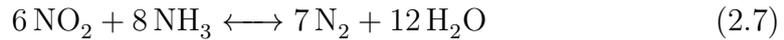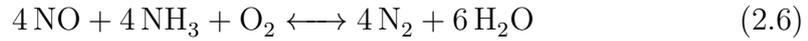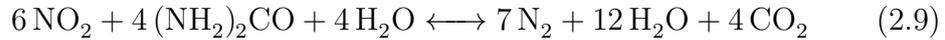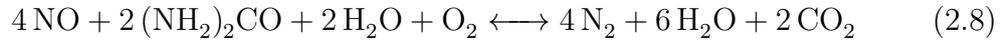
As shown in Figure 2.2 ammonia is taken from a storage tank, evaporated, mixed with air and injected into the flue gas, upstream of the catalyst. The conversion of NO_x occurs on the catalyst surface, which is made of metal oxides such as vanadium oxide. These active substances are coated on a basic material like zeolites [10, 1, 11]. There are three possible configurations for the implementation of the SCR reactor into the flue gas chain:

- **High-dust:** This installation option is the most common one. Here the SCR reactor is placed directly after the boiler, which leads to a high inlet temperature of the flue gas. Therefore, due to the high operating temperature of the catalyst, the flue gas reheating is avoided.
  However there is still the drawback of catalyst deactivation by fly ash and catalyst poisons, which are not removed from the flue gas at this point. This may lead to shorter catalyst lifetime.

- **Low-dust:** The drawback of the high-dust configuration is avoided by removing the particulate matter from the flue gas before entering the SCR reactor. This is done by an high temperature dust precipitator, so that there is no huge temperature drop. Due to the high equipment costs this process often proves to be uneconomic for retrofitting old power plants.

- **Tail-end:** For retrofitting existing plants this variant is favourable. Due to the installation at the end of the flue gas chain the catalyst is protected from abrasion, corrosion and deactivation.
  The drawback with this option, is that it needs a re-heater to reach the operating temperature of the catalyst and therefore energy, which leads to a decrease in efficiency.
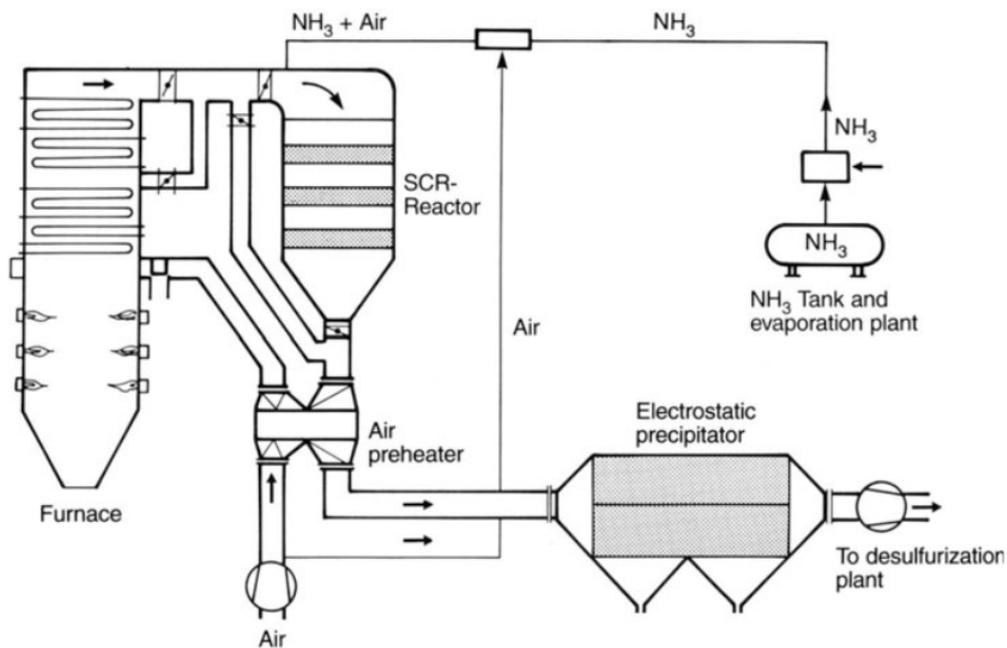
Figure 2.2: SRC process in the exhaust gas stream of a power plant furnace [11].

Oxidizing processes

Ozone processing: Ozone processing is used to oxidize nitrogen monoxide further, to get more soluble nitrogen compounds. Thus nitrogen oxide is converted into NO_2 and N_2O_5, both products are highly soluble in water and can be further treated by a wet process.

One technology that uses ozone for NO_x removal is named LoTOx^{TM}. Figure 2.3 illustrates the simplified process diagram for the concept. The required ozone is directly produced on site and on demand by passing oxygen through an ozone generator. That means that the O_3 is generated in response to the amount of NO_x present in the exhaust gas. The Ozone then rapidly reacts with the NO and results in NO_2 and N_2O_5 (according to the Reactions 2.10, 2.11) which is afterwards removed by wet scrubbers where HNO_3 is formed (Reaction 2.12) [33].

$$NO + O_3 \longrightarrow NO_2 + O_2 \tag{2.10}$$

$$2\,NO_2 + O_3 \longrightarrow N_2O_5 + O_2 \tag{2.11}$$

$$N_2O_5 + H_2O \longrightarrow 2\,HNO_3 \tag{2.12}$$
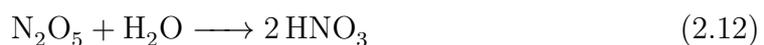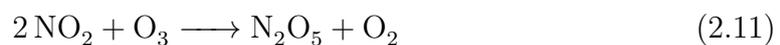
The LoTOx^{TM} process is in the early commercial state. The technology has been implemented, for demonstration, into the exhaust gas stream of the Medical College of Ohio (MCO) power plant (25 MW) in 2001. Furthermore, commercial experience was gained in the metal pickling process (see Table 2.1) as well as in the refinery industry [34].
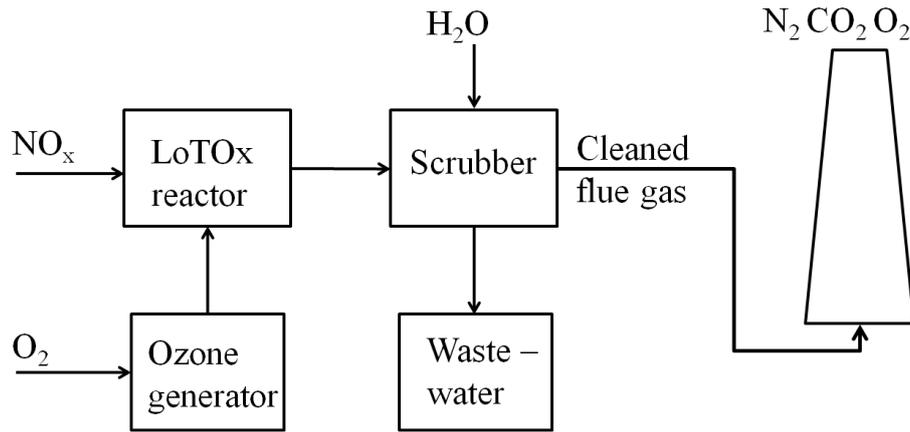
Figure 2.3: Simplified process diagram of the LoTOx$^{\text{TM}}$ concept.

Table 2.1: Commercial applications of the LoTOx$^{\text{TM}}$ technology [34].

Application	Location	Flue gas stream m^3 h^{-1}	NOx - in / out ppm
Metal Pickling Process	Pennsylvania	7650	3400 / 100
Natural gas-fired boiler	California	13600	150 / 2 − 5
Lead recovery furnace	California	42500	50 / 10

LICONOX®: Another secondary option based on oxidation of NO was proposed by LINDE especially for oxy-fuel combustion processes. The oxy-fuel combustion is used for carbon capture and storage (CCS) and therefore a highly concentrated CO$_2$ stream with low impurities is necessary. This is achieved by using oxygen instead of air for the combustion process. However the nitrogen and sulphur, which are naturally present in the fuel, form NO$_X$ and SO$_X$ during the oxidation and flue gas compression process. The presence of these impurities may lead to acid formation in the compression section and can thus cause material damage. Therefore and to achieve the strict purity standards for CCS the NO$_x$ and SO$_x$ need to be separated [3, 5, 6].

The developed NO$_x$ removal method, so called LICONOX® (Figure 2.4), uses that gas-phase reactions, are often faster at high pressures. Even at 10 bar NO converts, when oxygen is present, to the soluble NO$_2$ of its own accord. As it is necessary, for the CO$_2$ separation process, to compress the flue gases the step of high pressure NO$_x$ removal can be established without special effort.

Another advantage of this process is gained through adding ammonia solution. This reacts with the nitrogen dioxide and forms ammonium nitrate as well as ammonium nitrite according to the reaction 2.13 and 2.14, both forming the basis for liquid fertilisers, a usable by-product [3, 4].

$$NO + NO_2 + 2\,NH_3 + H_2O \longrightarrow 2\,NH_4NO_2 \qquad (2.13)$$

$$2\,NO_2 + 2\,NH_3 + H_2O \longrightarrow NH_4NO_2 + NH_4NO_3 \qquad (2.14)$$
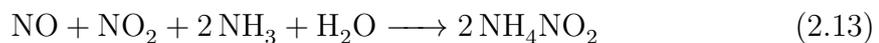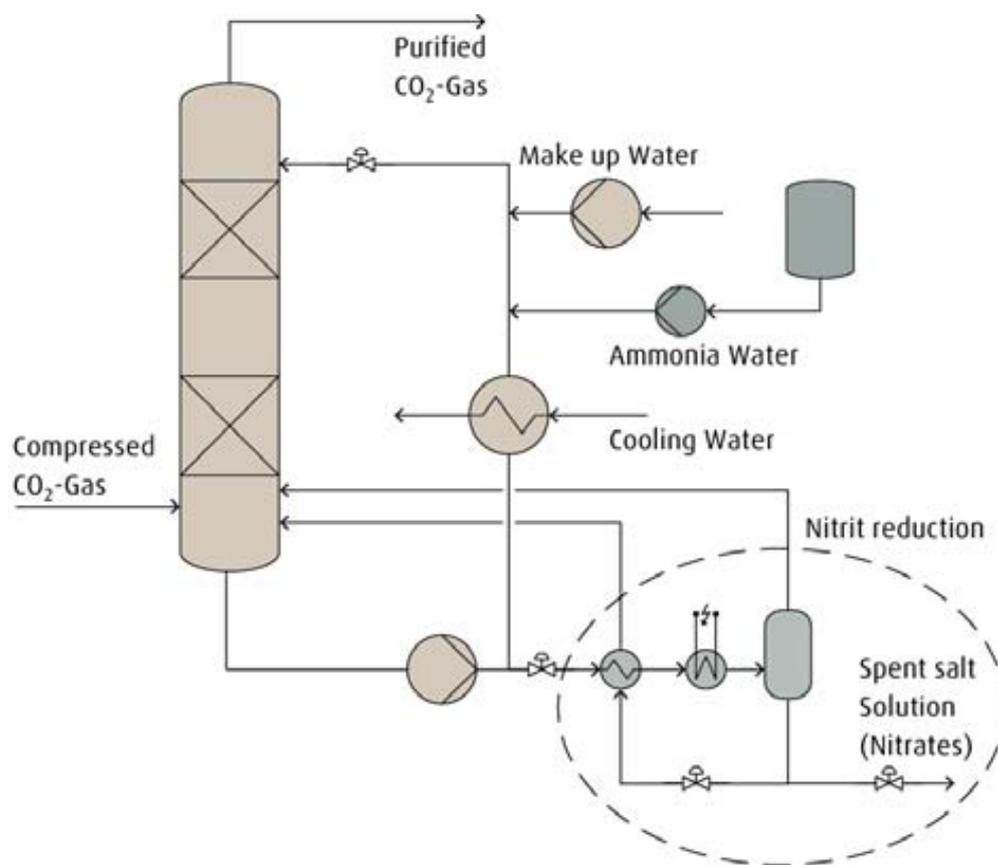
Figure 2.4: Flow diagram of the LICONOX® process [4].

2.2.3 Summary

Table 2.2: Overview of the before mentioned NO_x removal options [4, 11, 12, 35, 33, 34, 40].

Technique	Efficiency of NO_x removal	Performance parameter		Remarks[1]	Costs[3]
		Parameter	Value		
SNCR	30% – 80%	Operating temperature: Reducing agent: NH_3-slip: NH_3/NO_x ratio:	900 °C – 1100 °C Ammonia, urea < 10mg Nm^{-3} 1.5 – 2.5	− Common efficiency range only up to 50% − Cannot be used for gas turbines or engines − Incomplete reaction between NH_3 and NO_x leads to ammonium sulphate formation and deposition on downstream facilities, increased amount of NH_3 in the flue gas and the fly-ashes	Capital: 1.8 M€ Operating: 12.5 k€ yr^{-1}
SCR	85% – 95%	Operating temperature: Reducing agent: NH_3-slip: NH_3/NO_x ratio:	250 °C – 500 °C Ammonia, urea < 5mg Nm^{-3} 0.8 – 1.0	+ Incomplete NH_3-NO_x-reaction unlikely − Life of catalyst 6 – 12 years depending on the combusted fuel + By periodical washing lifetime can be increased	Capital: 9.8 M€ Operating 12.5 k€ yr^{-1}
LoTOx™	< 95%	Operating temperature: Oxidizing agent: O_3-slip: O_3/NO_x ratio:	65 °C – 135 °C Ozone 0 < 2.0	+ No NH_3-slip + Simultaneous NO_x and SO_x reduction	Capital: 32 – 64 € kW^{-1} [2]
LICONOX®	> 75%	Operating temperature: Oxidation:	30 °C – 120 °C Pressure	+ No additional chemicals needed + Cheap (high pressure needed for CCS anyways)	No data available

1): − for negative points; + for positive points

2): only data for capital costs available, cause of early commercial state

3): **data for SNCR and SCR on basis of a 100 MW refinery combustion plant [12]**

2.3 Chemistry of Cl − N − S system

The flue gas cleaning process with ClO_2 combines both gas- and liquid-phase chemistry of chlorine, nitrogen and sulfur reactions and interactions, here called Cl − N − S system. The main gas-phase reactions are taking part in the oxidizer. In the following step within the so called absorber, reactions in the gas- and liquid-phase as well as transport mechanisms are involved. The basis of these reactions are discussed in this chapter.

2.3.1 Film theory

For absorption processes the *two film theory* is commonly used, which was proposed by Whitmann in 1924 [51]. The basis for this theory is the assumption that the bulk phases are perfectly mixed and all transport resistance is located in two thin films near the interface (compare Figure 2.5). Furthermore it can be assumed that the interface is at equilibrium. Therefore all transport resistance occurs when the molecule is diffusing through the gas and liquid films. The flux through both layers has to be the same because of mass balance [53]. For the concentrations at the interface Henry's constant (defined in Equation 2.16) is valid. The resulting overall equation for the mass flux is given in Equation 2.15 with the total velocity calculated with Equation 2.17 [52]. Henry's constant can be defined in different ways, the one used in Equation 2.16 describes the volatility of the pollutant and is dimensionless.
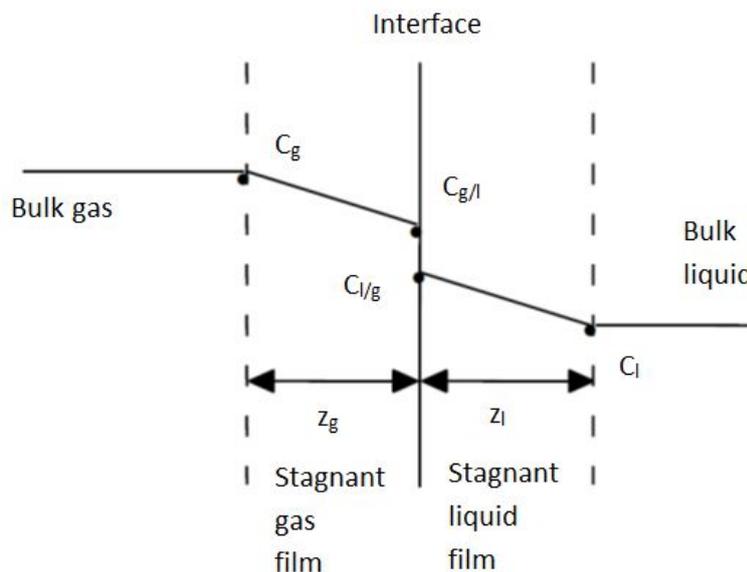
Figure 2.5: Visualisation of two film theory [53].

$$F = v_{tot} \left(C_l - \frac{C_g}{K_H} \right)$$

(2.15)

$$K_H = \frac{C_{g/l}}{C_{l/g}} \tag{2.16}$$

$$v_{tot} = \frac{1}{\frac{z_L}{D_l} + \frac{z_g}{D_g K_H}} \tag{2.17}$$

F	:	Mass flux / kmole m^{-2}s^{-1}
v_{tot}	:	Total velocity / m s^{-1}
C_l	:	Concentration of pollutant in liquid / kmole m^{-3}
C_g	:	Concentration of pollutant in gas / kmole m^{-3}
K_H	:	Henry's volatility constant / $-$
$C_{g/l}$	:	Equilibrium concentration of pollutant in gas / kmole m^{-3}
$C_{l/g}$	:	Equilibrium concentration of pollutant in liquid / kmole m^{-3}
z_l	:	Thickness of liquid layer / mm
D_l	:	Diffusivity of pollutant in liquid / m^2 s^{-1}
z_g	:	Thickness of gas layer / mm
D_g	:	Diffusivity of pollutant in gas / m^2 s^{-1}

After the mass transfer liquid-phase chemistry consists mainly of two kinds of reactions. The reactions of the dissolved pollutants with water and acid dissociation, where the formed acids dissolve in ions. The other reactions are interaction reactions between the different acids or pollutants.

2.3.2 Reactions of Cl − N − S

The oxidation of nitrogen oxide has been widely studied and is well understood [7, 8, 33]. Most of these studies describe the nitrogen oxide removal by using different oxidation agents (e.g. ozone) as well as different process conditions. Ajdari et al. [5, 6] mentioned the advantage of high pressure and low temperature to the NO oxidation as well as the increase of possible reactions between the nitrogen- and sulfur-species when SO_x is present. Further studies describe the reactions by using aqueous chlorine dioxide solution for a simultaneous removal of SO_2 and NO [30, 32].

In Figure 2.6 an overview to the most important reactions in the gas and liquid phase are presented. The absorption of SO_2 in the liquid phase may lead to the formation of sulfuric acid and N-S complexes. These reactions are highly dependent of the pH level of the solution. N-S complexes are build by the interaction between dissolved NO_2^- and HSO_3^-. This reaction results in different possible pathways depending on the pH level of the liquid, illustrated as red and white colored paths in Figure 2.6. Whereas the red path takes place at low pH-values (below pH $= 2$) and should be avoided because of its N_2O formation. N_2O is a strong greenhouse gas which stays for a long time in the atmosphere, because it has no natural sinks. At pH levels around four and higher the white pathway is predominant and no N_2O is formed. Therefore this way should be preferred [14, 39].
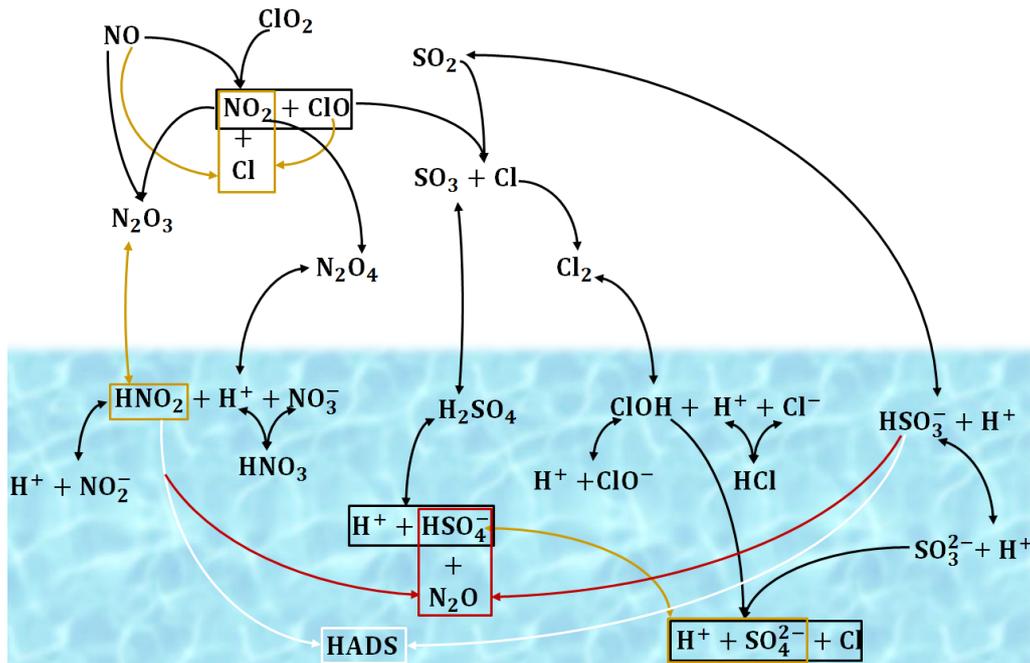
Figure 2.6: Simplified illustration of possible reactions in gas and liquid phase (HADS: hydroxylamine disulfonic acid). Red path: for pH-values lower than 2; White path: at pH-values around 4

2.4 ASPEN PLUS

The main purpose of the simulation model is to evaluate the design of the removal concept for different flue gas streams and therefore a sensitivity analysis of the concept. This is necessary to be able to compare the process with other removal options later on. For this task the commercial simulation software ASPEN PLUS V8.2 is used. This process simulation tool is an advanced steady state flowsheeting program and can be used for conceptual design, performance monitoring and optimization of various processes. With the large database of pure component and equilibrium data ASPEN PLUS is able to handle chemical conversion reactions. Furthermore transport phenomena can be included. That provides the opportunity to handle mass and energy balances. Therefore the determination of necessary sizes of process equipment like absorbers is possible.

To enable a better understanding of simulation, a summarizing description of the used ASPEN tools for the reactor is given.

2.4.1 Reactor

ASPEN provides a large spectrum of reactor types. In this work the REquil and RCSTR have been tested.

Reactor REquil

The REquil model is a rigorous equilibrium reactor, based on reaction stoichiometry. Rigorous means, that it is necessary to define the reactions which should be considered in the reactor. For the calculation of the product stream flow rates REquil uses the equilibrium constants, which are determined from Gibbs free energy. A basis for the equilibrium constants is given by the user-specified reaction stoichiometry and the yield distributions [37].

Reactor RCSTR

The RCSTR model is also a rigorous reactor with rate-controlled reactions, based on specified kinetics. Equilibrium reactions can be modeled simultaneously with rate based reactions. Furthermore perfect mixing within and between the phases, phase equilibrium, isothermal and isobaric operation is assumed by the reactor. The hold-up can be defined in several ways. In this work it is done by setting a total residence time of the flue gas inside the reactor [37].

As mentioned before, RCSTR uses rate-controlled reactions. For these the kinetic data has to be specified. Thus a built-in power law expression, compared to equation 2.18 for specified and 2.18 for unspecified reference temperature, is provided by ASPEN. At this point mentioned equation is given for the concentration basis *molarity* selected in the ASPEN sheet *kinetic*. Furthermore the unit of the reaction rate depends on the order of the reaction. As all given reactions are of the second order the valid units for the setup are listed below [37].

$$r = k \left(\frac{T}{T_0}\right)^n e^{-\left(\frac{E}{R}\right)\left[\frac{1}{T} - \frac{1}{T_0}\right]} \prod_{i=1}^{N} C_i^{\alpha_i} \tag{2.18}$$

$$r = kT \, e^{-\left(\frac{E}{R}\right)\frac{1}{T}} \prod_{i=1}^{N} C_i^{\alpha_i} \tag{2.19}$$

r	:	Rate of reaction / kmole m^{-3} s^{-1}
k	:	Pre-exponential factor / m^3 kmole^{-1} s^{-1}
T	:	Absolute temperature / K
T_0	:	Reference temperature / K
n	:	Temperature exponent / -
E	:	Activation energy / J mole^{-1}
R	:	Gas law constant / J K^{-1} mole^{-1}
$\prod$	:	Product operator / -
N	:	Number of components / -
C_i	:	Concentration of the ith component / kmole m^{-3}
α_i	:	Exponent of the ith component (here 2, second order reaction)

3

Reactions

In this chapter the reactions for the later on modeling are identified.

3.1   Gas-phase reaction mechanism

Important gas-phase reactions and their kinetics are presented in Tables 3.1, 3.2 and 3.3. The parameters for the rate expression are given in the form ASPEN uses it (compare Equation 2.18 in section 2.4.1).

Table 3.1: Reaction kinetic of NO reactions in the gas phase for a reference temperature of 298 K.

Reaction	k $\text{m}^3\ \text{kmole}^{-1}\ \text{s}^{-1}$	n –	E J mole^{-1}		Reference
$NO + ClO_2 \longrightarrow NO_2 + ClO$	$6.62 \cdot 10^7$	–	-2910	(3.1)	[15]
$NO + ClO \longrightarrow NO_2 + Cl$	$3.73 \cdot 10^9$	–	-2450	(3.2)	[16]
$Cl + ClO_2 \longrightarrow 2\,ClO$	$1.93 \cdot 10^{10}$	–	-1413	(3.3)	[9]
$2\,ClO \longrightarrow ClO_2 + Cl$	$2.11 \cdot 10^8$	–	11330	(3.4)	[9]
$NO + HCl \longrightarrow HNO + Cl$	$1.58 \cdot 10^{10}$	–	210000	(3.5)	[23]
$NO_2 + HCl \longrightarrow HNO_2 + Cl$	$3.98 \cdot 10^8$	–	98110	(3.6)	[28]
$NO + NO_2 \longleftrightarrow N_2O_3$	–	–	–	(3.7)	[31]
$2\,NO_2 \longrightarrow N_2O_4$	$5.00 \cdot 10^8$	-1.1	–	(3.8)	[25]
$N_2O_4 \longrightarrow 2\,NO_2$	$7.83 \cdot 10^{15}$	-3.8	53120	(3.9)	[26]
$2\,NO + O_2 \longrightarrow 2\,NO_2$ (reaction order 3)	$1.99 \cdot 10^{-15}\ ^{1)}$	–	-4410	(3.10)	[7]

1) different unit: $\text{cm}^6\ \text{mole}^{-2}\ \text{s}^{-1}$

Table 3.2: Reaction kinetic of SO_2 reactions in the gas phase for a reference temperature of 298 K.

Reaction	k m^3 $kmole^{-1}$ s^{-1}	n –	E J $mole^{-1}$		Reference
$SO_2 + ClO \longrightarrow SO_3 + Cl$	2409	–	–	(3.11)	[19]
$SO_2 + NO_2 \longrightarrow SO_3 + NO$	$6.31 \cdot 10^9$	–	27000	(3.12)	[22]
$4 SO_2 + 2 ClO_2 \longrightarrow 4 SO_3 + Cl_2$	–	–	–	(3.13)	[31]
$SO_2 + HOCl \longrightarrow SO_3 + HCl$	–	–	–	(3.14)	[31]
$SO_2 + 2 HNO_2 \longrightarrow H_2SO_4 + 2 NO_2$	–	–	–	(3.15)	[31]
$SO_2 + OH \longrightarrow HOSO_2$	$7.89 \cdot 10^8$	-0.7	–	(3.16)	[7]
$HOSO_2 + O_2 \longrightarrow H_2O + SO_3$	$7.83 \cdot 10^8$	–	2740	(3.17)	[7]

Table 3.3: Reaction kinetic of further Cl reactions in the gas phase for a reference temperature of 298 K.

Reaction	k m^3 $kmole^{-1}$ s^{-1}	n –	E J $mole^{-1}$		Reference
$2 Cl \longrightarrow Cl_2$ (reaction order 3)	$5.802 \cdot 10^{8}$ [1]	–	-6690	(3.18)	[21]
$Cl_2 + H_2O \longrightarrow HCl + HOCl$	–	–	–	(3.19)	[31]
$H_2O + Cl \longrightarrow OH + HCl$	$1.17 \cdot 10^8$	1.67	63850	(3.20)	[20]
$HNO_3 + Cl \longrightarrow NO_3 + HCl$	$9.03 \cdot 10^9$	–	36420	(3.21)	[24]
$NO_2 + ClO \longrightarrow ClNO_3$ (reaction order 3)	$5.94 \cdot 10^{10}$ [1]	-3.4	–	(3.22)	[9]
$ClNO_3 \longrightarrow NO_2 + ClO$	$1.66 \cdot 10^{15}$	–	94780	(3.23)	[27]
$ClNO_3 + Cl \longrightarrow Cl_2 + NO_3$	$3.73 \cdot 10^9$	–	-1210	(3.24)	[9]

[1] different unit: cm^6 $mole^{-2}$ s^{-1}

Assumptions for gas-phase reactions

To keep the simulation model as simple as possible, the most important reactions had to be identified. This is done especially for the NO reactions, by calculating the reaction rates for a typical process concentration of each component in the gas (see Table 3.4). Figure 3.1 represents the results of this calculation.

Table 3.4: Considered gas composition for reaction rate calculation.

	NO	NO_2	N_2O_4	ClO_2	ClO	Cl	HCl	H_2O	O_2
Value / ppm	125	125	100	35	35	70	100	50000	40000
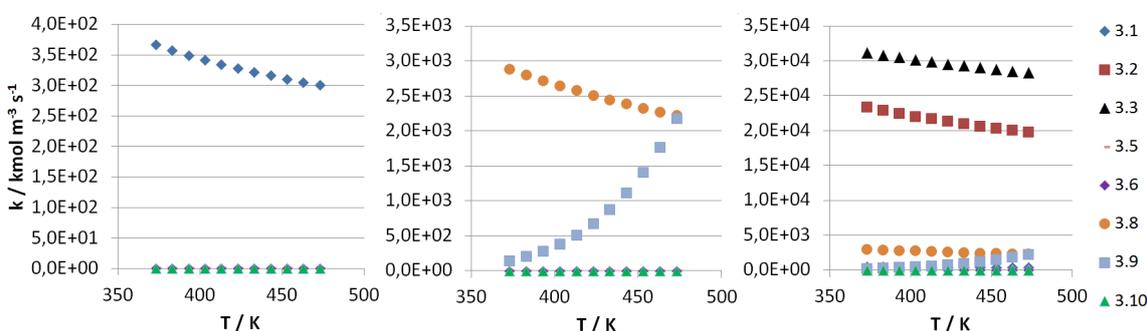
Figure 3.1: Reaction kinetic of selected reactions over a temperature range of 373 – 473 K.

NO reactions: The most important reactions for nitrogen oxide in the gas-phase are 3.1 and 3.2. Both reaction kinetics are really fast (see left and right plot in Figure 3.1). Another reason for implementing these reactions into the ASPEN PLUS model are their reactants ClO_2 and ClO. Chlorine dioxide is the oxidation agent used for NO oxidation and chlorine monoxide is a product out of reaction 3.1 and 3.3. Thus the NO oxidation reactions 3.1 and 3.2 as well as the chlorine dioxide and its reverse reaction (3.3, 3.4) are implemented into the model.

The Reactions 3.5 and 3.6 are not taken into account. This is caused by the fact that the reaction rates for both are low. Thus there is no significant product forming taking part during the residence time in the reactor (compare Figure 3.1). Reaction 3.7 is mentioned as an major one taking part in the gas-phase in [31]. It is also noted as an equilibrium reaction. Both Reactions 3.8 and 3.9 are implemented into the model. The first one is not only important because of its fast reaction rate, but also of the solubility of its product (N_2O_4). The back reaction is takes part especially at higher temperatures (center plot of Figure 3.1). Reaction 3.10 is possible in the gas-phase, but really slow in the temperature range of the reactor (373 – 473 K) (see Figure 3.1) and can therefore be neglected for the reactor.

SO_2 reactions: Reaction 3.11 is the only SO_2 reaction with the oxidation agent ClO_2 or a compound of it, here ClO. For that reason it is the most important reaction for sulfur dioxide in the gas-phase and therefore implemented into the simulation model. No direct reaction of SO_2 with chlorine dioxide could be found. The Reactions

3.13 until 3.15 as well as the Cl Reaction 3.19 are only mentioned by J. J. Kaczur as theoretically possible, but no kinetic information has been reported [31]. Therefore this mechanisms are neglected in the simulation model. Reactions 3.16 and 3.17 are based on radical forming out of H_2O due to Reaction 3.20. This is significant at much higher temperatures. The reactor is used at much lower temperatures (around 373 – 473 K), thus this reaction chain is not taken into account.

Reaction 3.12 is the interaction reaction between SO_2 and NO_2 in the gas phase. This reaction is slow in the temperature range of the reactor (373 – 473 K) and can therefore be neglected for the modelling.

Cl reactions: For the chlorine chemistry only the reaction 3.18 is taken into account. The reverse reaction of 3.18 is significant at much higher temperatures than 373 – 473 K. Thus only the forward one was implemented into the model. For the other reactions not all reactants are present in the system and therefore the reactions are not able to react. The reaction rate of Reaction 3.22 is very slow and therefore not significant during the residence time in the reactor[9].

3.2 Liquid-phase reaction mechanism

Section 2.3.2 deals with the possible liquid phase reactions in the absorber. To reduce the simulation time and the error probability some unimportant reactions were neglected. This is discussed in the following chapters, showing the used reactions. Many of the used reactions are equilibrium reactions, these are put in aspen by equation 3.25. For kinetic reactions applies Equation 2.19

$$ln(K_{eq}) = A + \frac{B}{T} + C \cdot T \tag{3.25}$$

K_{eq} : Equilibrium constant / kmole m^{-3}
T : Absolute temperature / K
A : User supplied coefficient / -
B : User supplied coefficient / K
C : User supplied coefficient / K^{-1}

Table 3.5: Important liquid-phase reactions of nitrogen oxides.

Reaction	k m^3 $kmole^{-1}$ s^{-1}	n –	E J $mole^{-1}$	ref. Temp °C		Reference
$2NO_2 + H_2O \longrightarrow HNO_2 + H^+ + NO_3^-$	$1.0 \cdot 10^8$	–	–	22	(3.26)	[46]
$2\,HNO_2 \longrightarrow NO + NO_2 + H_2O$ "	13.4	–	–	22	(3.27)	[48]
$NO + NO_2 + H_2O \longrightarrow 2\,HNO_2$	$1.58 \cdot 10^8$	–	–	22	(3.28)	[48]

Reaction	A –	B –	C –	ref. Temp °C		Reference
$N_2O_4 \longleftrightarrow HNO_2 + HNO_3$	26.522	–	–	25	(3.29)	[57]
$HNO_3 \longleftrightarrow H^+ + NO_3^-$	6.908	–	–	25	(3.30)	[44]
$HNO_2 \longleftrightarrow H^+ + NO_2^-$	-7.684	–	–	25	(3.31)	[44]

": Reaction not considered

Table 3.6: Important liquid-phase reactions of sulfur oxides.

Reaction	A –	B –	C –	ref. Temp °C		Reference
$SO_2 + H_2O \longleftrightarrow H^+ + HSO_3^-$	-5.979	637.396	-0.0151	20	(3.32)	[60]
$HSO_3^- \longleftrightarrow H^+ + SO_3^{2-}$	-25.291	1333.4	–	20	(3.33)	[60]
$SO_3 + H_2O \longleftrightarrow H_2SO_4$	55.04 [1)]	–	–	25	(3.34)	[54]
$H_2SO_4 \longleftrightarrow H^+ + HSO_4^-$	6.908	–	–	25	(3.35)	[44]
$HSO_4^- \longleftrightarrow H^+ + SO_4^{2-}$	-4.423	–	–	25	(3.36)	[44]

1): incomparable high, results in a simulation error, computed from Gibbs energies instead

Table 3.7: Simplified interaction reactions between HNO_2 and HSO_3^-.

Reaction	k m^3 kmole^{-1} s^{-1}	n –	E J mole^{-1}	ref. Temp °C		Reference
$HNO_2 + HSO_3^- \longrightarrow HSO_4^- + 0.5N_2O + 0.5H_2O$	$1.887 \cdot 10^9$	–	50718.22	–	(3.37)	[21]
$HNO_2 + 2\,HSO_3^- \longrightarrow HADS + H_2O$	$1.887 \cdot 10^9$	–	50718.22	–	(3.38)	

Table 3.8: Important liquid-phase reactions of chlorine compounds.

Reaction	k m^3 kmole^{-1} s^{-1}	n –	E J mole^{-1}	ref. Temp °C		Reference
$2\,Cl \longrightarrow Cl_2$	$8.75 \cdot 10^7$	–	–	23	(3.39)	[45]
$ClOH + SO_3^{2-} \longrightarrow SO_4^{2-} + 2\,H^+ + Cl^-$ "	–	–	–	25	(3.40)	[49]

Reaction	A –	B –	C –	ref. Temp °C		Reference
$Cl_2 + H_2O \longleftrightarrow CLOH + H^+ + Cl^-$	-11.375	-1286.97	–	20	(3.41)	[60]
$HCl \longleftrightarrow H^+ + Cl^-$	-8.775	6896.24	–	25	(3.42)	[44]
$ClOH \longleftrightarrow H^+ + ClO^-$	-16.152	-1602.87	–	20	(3.43)	[60]

": Reaction not considered

Assumptions for liquid-phase reactions

NO reactions: The decomposition of HNO_2 is quite slow and its back reaction much faster so the decomposition can be neglected in this case [48]. To test this assumption some simulations were tested with and without the decomposition reaction and the difference of HNO_2 amount in the exhaust gas as well as in the absorber water outlet was below 1%.

SO reactions: The coefficient values of reaction 3.32 and 3.33 are computed with the electrolyte wizard of aspen plus. The coefficient of the other reactions are found in literature. As can be seen by the low coefficients in Table 3.6 the dissociation of HSO_3^- is quite low which is important for the assumptions for Cl reactions. The dissociation reaction was taken into account anyhow for stages with higher pH-value.

Interaction reactions between HNO_2 and HSO_3^-: The simplified reactions between HNO_2 and HSO_3^- are given in Table 3.7. For a pH-value around one and below only reaction 3.37 should be used, for a pH-value around four and above only Reaction 3.38 takes place. The pH-value in the relevant stages, where both HNO_2 and HSO_3^- is present, is between one and four, what makes it necessary to use both equations. Because the pH-value is mainly around 2.5 in the mentioned stages, the assumption that both interaction reactions take place equally is valid. As written in section 2.3.2 the pH-value of four would be favourable, but at the same time more water and thus a bigger absorber would be needed. The kinetics in Table 3.7 are based on the rate expression without defined reference Temperature (compare equation 2.19).

Cl reactions: Reaction 3.40 can be neglected because of the low SO_3^{2-} content, due to the low pH-value. HSO_3^- is a moderately week acid, so with many H^+ ions present there is, as mentioned in the SO reactions paragraph, hardly HSO_3^- dissociation (Reaction 3.33) [44].

4

Simulation model

In this chapter the simulation conditions for the oxidizer and the absorber model are discussed. Also the chemistry implemented into the models is presented.

4.1 Model of the oxidizer

The simulation of the oxidizer investigates the effect of operating conditions on NO conversion to higher nitrogen oxide compounds. Process conditions are changed, according to Table 4.1. The ranges of the parameters are inspired by normal flue gas concentrations of power and incineration plants. The typical exhaust gas compositions are listed in Table 4.2.

Table 4.1: Process conditions used in the experiments.

Condition	Value
NO / ppm	250
SO_2 / ppm	0, 350, 700
O_2 / %	4
CO_2 / %	17
N_2 / %	Balanced
Reactor temperature / °C	100 and 180
Residence time in reactor / s	1.65, 2.30, 3.00
Humidity in flue gas / vol.%	0
ClO_2 gas addition / mol $mol_{NO_x}^{-1}$	$0.2 - 0.8$

Table 4.2: Typical exhaust gas compositions [42].

Component	NO_x ppm	SO_2 ppm	O_2 %	CO_2 %	Humidity %
Coal power plant	$500 - 600$	$500 - 2000$	$5 - 9$	$15 - 18$	$10 - 15$
Oil power plant	$50 - 150$	$50 - 100$	$2.5 - 3.5$	$13 - 15$	n.a.
Waste incineration plant	$150 - 200$	$40 - 60$	$8 - 11$	$10 - 12$	n.a.

The parameters SO_2 and humidity were changed in three steps. The steps and ranges were selected so, that they reproduce the flue gas concentrations of the plants mentioned in Table 4.2. For the reactor simulations the flue gas humidity content was set to 0%. This is due to the fact that no gas-phase reactions with water were implemented (see set up section below). The other component values (NO, O_2, CO_2) stay constant. This is due to the fact that both O_2 and CO_2 are stable compounds and will not undergo a reaction in the used temperature range and residence time. NO was kept constant to achieve a better comparability. To keep the reactor dimensions low a maximum residence time of 3.00 s was selected.

NO or SO_2 conversion is defined as the reduction of these components. Calculated by comparing the amount at the inlet and outlet, Equation 4.1.

$$\text{NO/SO}_2 \text{ conversion} = 1 - \frac{\text{NO/SO}_2 \text{ out}}{\text{NO/SO}_2 \text{ in}} \tag{4.1}$$

For the oxidizer model (vapor phase) the ideal gas equation of state is used. This is valid due to the ambient pressure conditions in the reactor. ASPEN provides a large spectrum of reactor types. For this thesis the reactors REquil and RCSTR have been tested. Both are explained briefly in the theory part 2.4. The reason for taking these two ideal reactors is, that the main focus of this work is the chemistry and not the gas mixing and the reactor design. The used set up is explained below.

Set up

The specifications for both, the REquil and the RCSTR reactor model are summarized. In Table 4.3 the used reactions and the used controlling mechanisms are listed. Furthermore the utilized set up is given in Table 4.4.

For better comparison the first flue gas composition used in the simulation model is equal to the synthetic flue gas composition of the experiments which is listed in Table 4.1.

Table 4.3: Used reactions and controlling mechanisms in the simulation models.

Reaction		REquil-model	RCSTR-model
$NO + ClO_2 \longrightarrow NO_2 + ClO$	3.1	Equilibrium	Rate based
$NO + ClO \longrightarrow NO_2 + Cl$	3.2	Equilibrium	Rate based
$Cl + ClO_2 \longrightarrow 2\,ClO$	3.3	Equilibrium	Rate based
$2\,ClO \longrightarrow ClO_2 + Cl$	3.4	Equilibrium	Rate based
$SO_2 + ClO \longrightarrow SO_3 + Cl$	3.11	Equilibrium	Rate based
$2\,Cl \longrightarrow Cl_2$	3.18	Equilibrium	Rate based
$NO + NO_2 \longleftrightarrow N_2O_3$	3.7	Equilibrium	Equilibrium
$2\,NO_2 \longrightarrow N_2O_4$	3.8	Equilibrium	Rate based
$N_2O_4 \longrightarrow 2\,NO_2$	3.9	Equilibrium	Rate based

Table 4.4: Used set up for reactor simulation models in ASPEN PLUS.

Parameter	REquil-model	RCSTR-model
Valid phase:	Vapor-only	Vapor-only
Specification type:	–	Residence time
Residence time / s	–	1.65, 2.3, 3.0
Pressure / atm	1	1
Temperature / °C	100, 180	100, 180

4.2 Model of the absorber

The absorption which is taking part between the gas and water entering the absorber is accompanied by chemical reactions and therefore a so called reactive absorption. This is a complex rate-controlled process, so for the description of the process the equilibrium model is often not sufficient. Therefore the so called rate-based model, which involves the process kinetics, is required. The rate-based model considers besides the chemical reactions the actual rates of mass and heat transfer. For this usually the two-film model is used, which is explained in Section 2.3.1.

However it must be considered that there will be large uncertainties in the absorber simulation results and thus in the later on results of the whole system. This is due to the fact, that the present study is a conceptual study of the chemistry rather than aiming at predicting the exact behaviour of the absorber.

4.2.1 Absorber specifications

As absorber device a packed tower is selected. Packed towers are filled with packing materials, in this case Raschig ceramic rings (good acid resistance), to enlarge the surface area. The Raschig ring diameter is chosen to 15 mm, which results in a packing factor of 1250 m^{-1}. The advantage of the packed tower is the higher removal efficiency (i.e. less water is needed for more pollutant removal) and the higher possible liquid rate. The disadvantage is the more difficult and more expensive maintenance, as well as the higher pressure drop [50]. Further absorber specifications are given in Table 4.5. The tested flue gas compositions are listed in Table 4.6. The used reactions are already given in Section 3.2.

Table 4.5: Used set up for absorber simulation models in ASPEN PLUS.

Parameter	Cooler	RadFrac
Type:	Plate heat exchanger [1]	Packed tower
Valid phase:	Vapor-Liquid	Vapor-Liquid
Specification type:	Outlet temperature	Packing rating
Number of Plates/Stages:	156 [1]	50
Water mass-flow /10^6 kg hr^{-1}	3,078	0.5/3.6/5.2/9.5
Pressure / atm	1	1
Temperature (outlet) / °C	20	20
Area / m^2	1248	490
Height / m	8 [1]	70 [2]
Width/Diameter / m	1 [1]	25

1): example type and set up not affecting the simulation

2): first estimation

Table 4.6: Tested conditions for the absorption.

Compound	SOx only	NOx only	NOx and SOx	Experimental
N_2 / %	75.465	75.385	75.450	75.437
CO_2 / %	17	17	17	17
O_2 / %	4	4	4	4
H_2O / %	3.5	3.5	3.5	3.5
SO_2 / ppm	349	0	349	349
SO_3 / ppm	1	0	1	1
H_2SO_4 / ppm	1	0	1	1
NO / ppb	0	44	44	44
NO_2 / ppm	0	50	50	50
HNO_2 / ppb	0	50	50	50
N_2O_4 / ppm	0	100	100	100
Cl / ppm	0	0	0	89
Cl_2 / ppm	0	0	0	11
ClO / ppm	0	0	0	30

The diameter results from the typical operation range for the gas velocity through the columns. This is 50 to 75% of the flooding velocity (for a liquid to gas ratio of 0.5 l m^{-3} (50% flooding) and 5 l m^{-3} (75% flooding)). The large diameter is also a reason for using a packed tower. They are routinely used for diameters of 10 m and more [58]. The height of the tower is in a first step overestimated and gets downsized later on, depending on the amount of water, to reach emission limits. The number of stages is chosen to 50 because it is sufficient for a stable efficiency. At the same time the calculation time is kept in an acceptable range. The absorbent enters in the 50th stage (top) and the flue gas in the first stage (bottom). The reactions discussed in subsection 3.2, take place between the second and the 49th stage (less

error-prone simulation). The L/G-ratio is also quite high compared to common SO_2 scrubbers, but as shown in Chapter 6 by using sodium hydroxide the SO_2 is removed more efficiently which results in less water amount required. The test condition is given by a flue gas flow of $1.013 \cdot 10^6$ m^3 hr^{-1} (value of the example power plant Nordyjlandsverket in design condition) and the composition coming from the reactor. The ClO$_2$/NO ratio of 0.50 is selected because almost all NO is converted at this point. The water flow later referred to as low (L/G-ratio = 3.6) is computed to reach the SO_x emission limit. The flue gas composition referred to as SO_x in Table 4.6 is used for that. The two higher flows (L/G-ratio = 5.2; L/G-ratio = 9.5) are chosen to show the effect of the water amount. Beside the comparison of the pollutant absorption with different water amounts, all amounts are additionally tested with different pH-values of the scrubbing water. For this NaOH is added to the water in ionized form, and only the water equilibrium reaction is allowed, so that only the pH-value is influenced. Furthermore the different water amounts are tested with HNO$_2$ added. The HNO$_2$ amount is based on the amount that is in the liquid outlet of the absorber without HNO$_2$ in the inlet of the scrubbing water. The different conditions for the absorption are summarized in Table 6.1. The compositions of the four different flue gases are given in Table 4.6. The influence of the different tested conditions are discussed in Chapter 6.

For the later on comparison of the simulated absorption process, with other absorption measures (desulfurisation), the liquid to gas ratio is used. This is one of the most important parameters for setting up an absorber. In Table 4.7 different measures for gas absorption as well as their liquid to gas ratio and removal efficiencies are presented. For common packed bed absorbers the maximum L/G-ratio is as low as 0.5, thus this ratio is used for the modelled absorber and the removal efficiencies of the different component groups are compared with the efficiency of common packed towers.

Table 4.7: Efficiency of different absorption measures and their corresponding common liquid to gas ratios [55, 56].

Measure	Liquid to gas ratio l m^{-3}	Efficiency %
Spray tower	$1.5 - 3$	$95 - 99$
Impingement plate	$0.4 - 0.7$	$90 - 99$
Packed bed	$0.1 - 0.5$	$95 - 99$

4.2.2 External cooler

To reach the favoured temperature in the absorber and to decouple the absorber from the reactor regarding the temperature an external cooler is set upstream the absorber. It cools the flue gas coming from the reactor down to 20 °C which improves the solubility of the pollutants (e.g. huge difference of NO_2 and N_2O_4 solubility between 25 °C and 40 °C) [47]. Besides that, the N_2O generation at 20 °C is lower than at higher temperatures [38].

For cooling the given amount of flue gas from 100 °C down to 20 °C, while allowing the cooling water only to get heated from 10 °C to 20 °C (can be used directly in the absorber) a heat exchanging area of about 1246 m^2 is needed (aspen short-cut calculated). For such a large area a gasketed plate heat exchanger would be an option. It is important to consider the acid resistance when choosing the plate and gasket material. For this area a possible set up for the heat exchanger is e.g. 156 heat exchanging plates with an area per plate of about 8 m^2 [59]. The consideration about type and set up of the heat exchanger will become necessary when an economic evaluation is performed, but has no impact on the present simulations.

5

Reactor performance

In this chapter the results of the reactor simulation model are presented and compared to the experimental ones. The effects of different flue gas conditions on NO and SO_2 conversion are discussed. The exact flue gas composition and reactor parameter used for the comparison is due to confidentiality not mentioned.

5.1 Evaluation of the reactor model

This section contains a comparison between reactor simulation and experimental results. All trials refer to a standard flue gas composition as well as predefined reactor parameter. Also the reactions mentioned in section 3.1 are implemented.
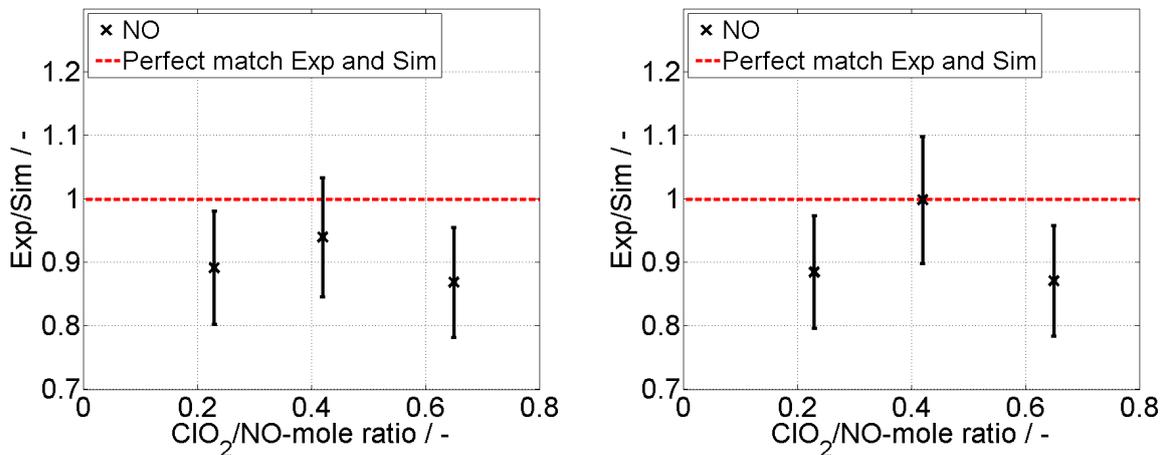
Figure 5.1: Normalized reactor validation results for NO for RCSTR-model (left) and REquil-model (right).

Comparison of NO conversion: In the first step the experimental conditions where used in the simulations to compare the gained NO conversion in the two cases. Thus the flue gas composition at the reactor inlet does not contain any SO_2 for this step. Figure 5.1 illustrates the experimental nitrogen monoxide conversion divided through the simulation results over different chlorine dioxide mole ratios. The plot on the left hand side compares the RCSTR reactor model with the experimental results, while the right graph shows the comparison of the REquil-model. Both models reproduce the gained outcomes of the experiment very well. The maximum deviation

is under 15% and by taking the measurement accuracy into account (error bars), there is only a slight deviation. The figures confirm that the models are suitable for NO conversion and the reactions are at equilibrium.

Comparison of SO₂ conversion: The results of this comparison step are only presented in the above mentioned tables. In the experiment there was no measurable conversion of SO_2 in the reactor, when no nitrogen oxide is present in the flue gas. This outcome is reproducible with both, the REquil and the RCSTR simulation model. Therefore both models showed to be suitable for SO_2 conversion, when no NO is present in the flue gas.
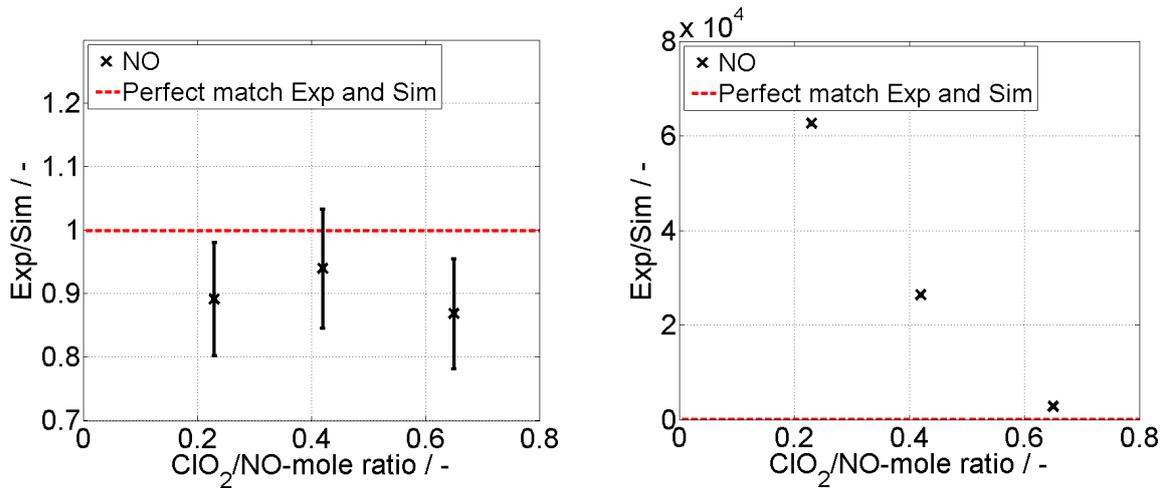
Figure 5.2: Reactor validation results for NO and SO_2 in flue gas, for RCSTR-model (left) and REquil-model (right).
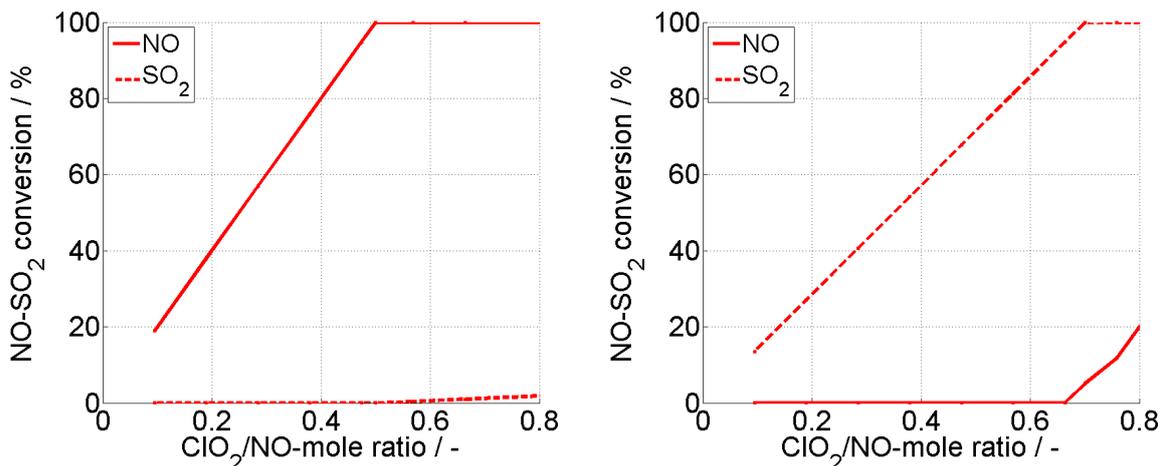
Figure 5.3: Reactor conversion results for NO and SO_2 in flue gas, for RCSTR-model (left) and REquil-model (right).

Comparison of NO and SO₂ conversion: The last step is to compare the experimental and simulation results when NO as well as SO_2 is present in the flue gas. As presented in Figure 5.2 (left), the NO conversion gained with the RCSTR-model fits to the experimental results. On the other side the results of the REquil-model is

completely different. Here first the SO_2 reduction takes place and the NO conversion does not start till the SO_2 is nearly totally reduced (5.3 right).

To sum up, it is not possible to describe the oxidation process with using just equilibrium reactions. The RCSTR-model also considers rate based reactions and is, as shown above, well suitable for the NO conversion. Due to the fact that the present study mainly deals with NO conversion in the Oxidizer, the RCSTR simulation model is considered as validated.

5.2 Simulation

This section deals with the results of the validated reactor model under different conditions. The gained data of the simulation are tabulated (see Table A.1 and A.2) in the Appendix A and only plots are used for the comparison of simulation and experimental results.

Effect of SO_2 content on NO and SO_2 conversion: The results are illustrated in Figure 5.4. Changing the SO_2 input content shows no effect on the NO conversion. Also the SO_2 conversion stays constant in a percentage kind of view. But the ppm amount which is converted rises with increasing the SO_2 content in the flue gas. The reason for this is by doubling the amount of SO_2 in the gas, also the reaction rate is doubled (function of concentration) and therefore the percentage conversion stays constant.

Furthermore the NO conversion is 100% at an ClO_2-NO mole ratio of 0.50, after which the SO_2 conversion starts.
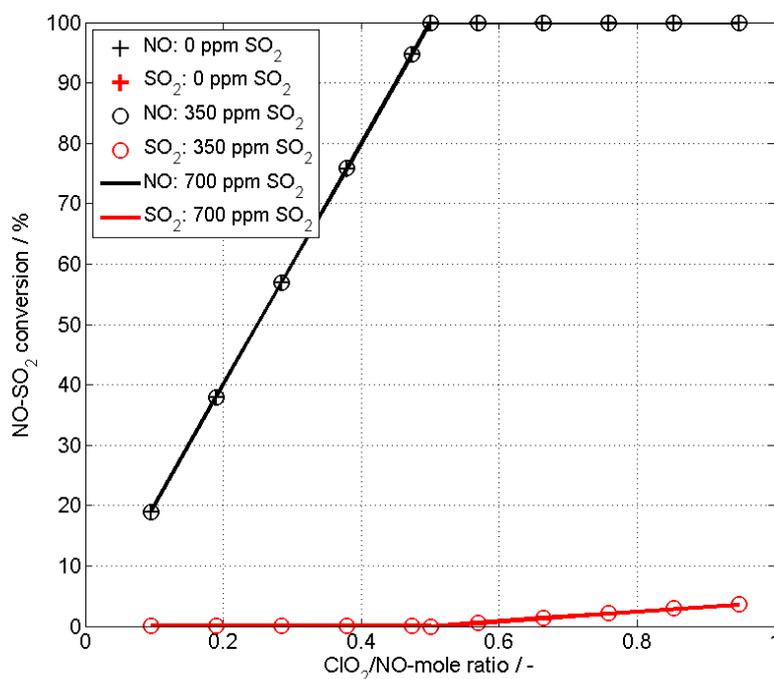
Figure 5.4: Effect of SO_2 content on NO and SO_2 conversion; $t_{res} = 1.65$ s; Flue gas composition: $NO_{in} = 250$ ppm, $H_2O_{in} = 0\%$.

Composition of nitrogen compounds at output: In Figure 5.5 the percentage composition of the nitrogen compounds at reactor outlet are illustrated. NO is constantly decreasing, until it is completely converted at a ClO_2/NO-ratio of 0.5. The NO_2 forming seems, with a range of 8 to 18%, to be quite low, what can be explained by the fact, that the N_2O_4 forming reaction (out of NO_2) has a high reaction rate (compare Section 3.1 Figure 3.1) and the NO_2 is converged into N_2O_4. No significant N_2O_3 amount is present.
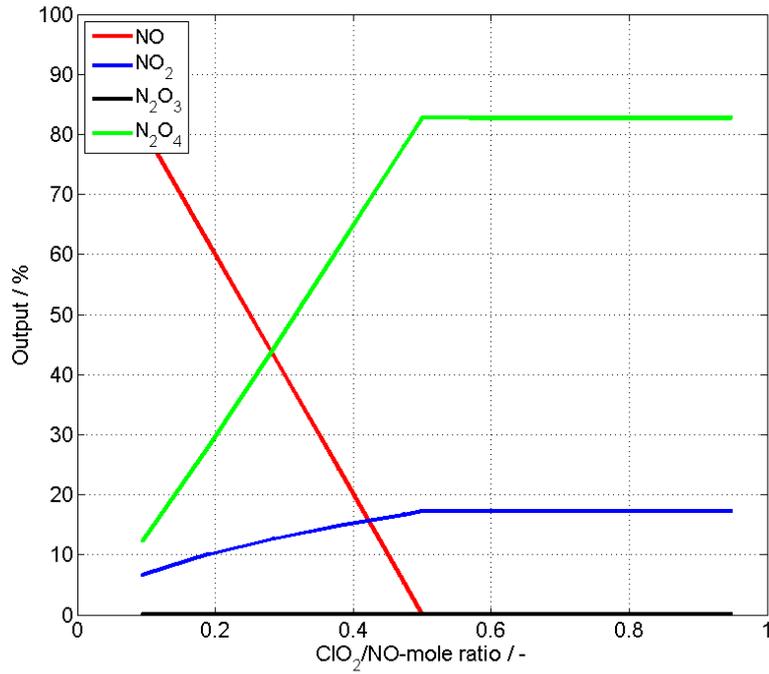
Figure 5.5: Composition of nitrogen compounds at output; $t_{res} = 1.65$ s; Flue gas composition: $NO_{in} = 250$ ppm, $SO_{2\ in} = 350$ ppm, $H_2O_{in} = 0\%$.
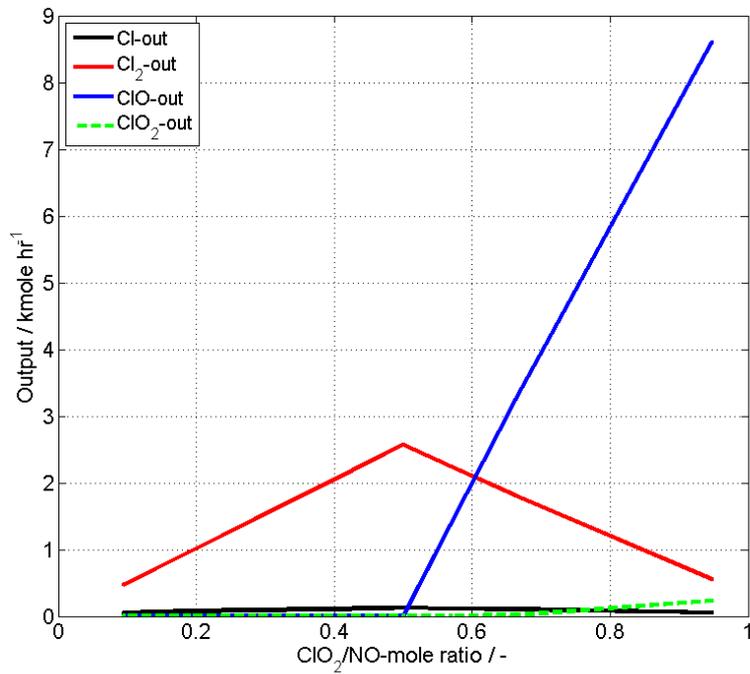
Figure 5.6: Effect of ClO_2-ratio on Cl compound output; $t_{res} = 1.65$ s; Flue gas composition: $NO_{in} = 250$ ppm, $SO_{2\ in} = 1000$ ppm, $H_2O_{in} = 0\%$.

Effect of ClO$_2$-ratio on Cl compound output: Figure 5.6 shows, that the reactor output on ClO is rapidly increasing, while Cl and Cl$_2$ output decreases with increasing ClO$_2$/NO-ratio. This happens at a ClO$_2$-NO mole ratio of around 0.5 and proceeds due to the fact, that at this point almost all NO is converted (see Figure 5.4). Thus more ClO$_2$ is available than needed, which leads to an increase in the reaction $Cl + ClO_2 \longrightarrow 2\,ClO$. The amount of ClO$_2$ is then at an value, that the reaction rate of the before mentioned reaction exceeds the rate of the $2\,Cl \longrightarrow Cl_2$ reaction. Therefore the CO$_2$ reactor output is decreasing, while the ClO output increases at a higher ClO$_2$/NO mole ratio than 0.5.
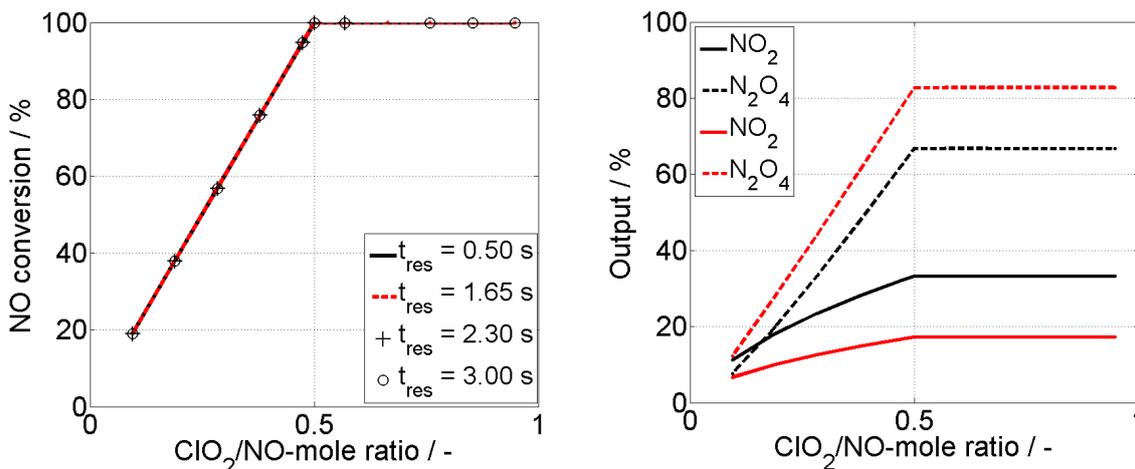
Figure 5.7: Effect of residence time on NO conversion (left) and NO$_2$, N$_2$O$_4$ output (right); colors: black $\widehat{=}$ t$_{res}$ = 0.50 s, red $\widehat{=}$ t$_{res}$ = 1.65 s; Flue gas composition: NO$_{in}$ = 250 ppm, SO$_{2\ in}$ = 350 ppm, H$_2$O$_{in}$ = 0%.

Effect of residence time on NO conversion: Another trail with a residence time of 0.50 s was progressed for achieving an effect on NO compound output. As illustrated in Figure 5.7 no difference in NO conversion between the tested reference times of 0.5, 1.65, 2.3 and 3.0 is visible. This is due to the fast reaction kinetics of:
$NO + ClO_2 \longrightarrow NO_2 + ClO$
$NO + ClO \longrightarrow NO_2 + Cl$
 The residence time has an effect on the N$_2$O$_4$ forming out of NO$_2$. Increasing the time from 0.50 to 1.65 s leads to an N$_2$O$_4$ increase of around 23% at the reactor outlet.

Effect of residence time on SO$_2$ conversion: The plots in Figure 5.8 show, that an increase in reactor residence time leads to a higher conversion of the incoming SO$_2$. This is explained by the slow SO$_2$ reaction kinetic. With an increase of 40% in residence time (1.65 s to 2.3 s) the SO$_2$ conversion enlarges of also almost 40%, while an increase of 80% (1.65 s to 3.0 s) just leads to an enlargement in SO$_2$ conversion of 75%. Thus further rises in time will lead to a stagnation eventually. This is caused by a decreasing availability of reactants and therefore also a decline in reaction rate.

Effect of temperature on NO conversion: As presented in Table 3.1 the activation Energy for the NO reactions with ClO and ClO$_2$ is negative. A rising temperature induces therefore in a decreasing reaction kinetic. The considered tem-
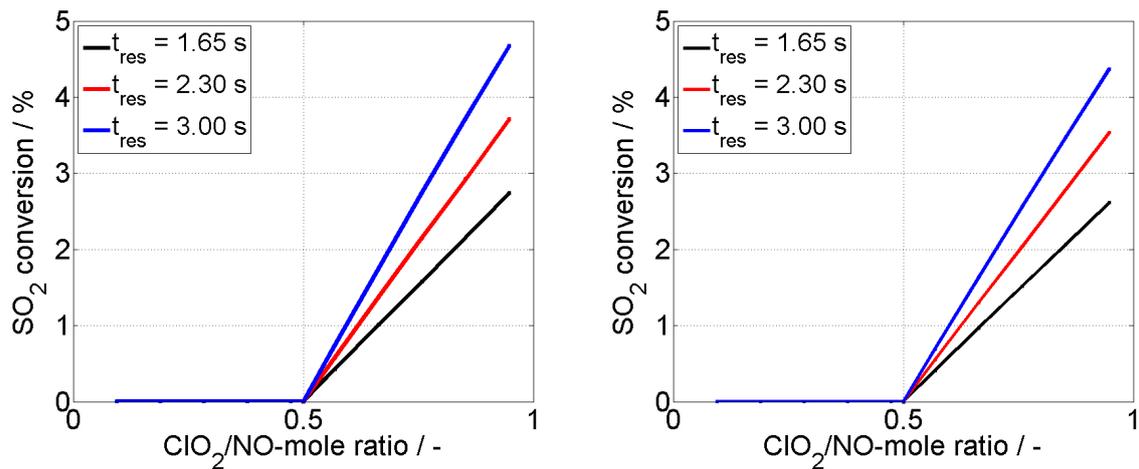
Figure 5.8: Effect of residence time on SO_2 conversion for 350 ppm SO_2 content (left) and 700 ppm SO_2 content (right).

perature rise in the reactor has only a slight effect on the reaction kinetic (see Figure 3.1) and thus, as illustrated in Figure 5.9, no visible effect on the NO conversion inside the reactor.
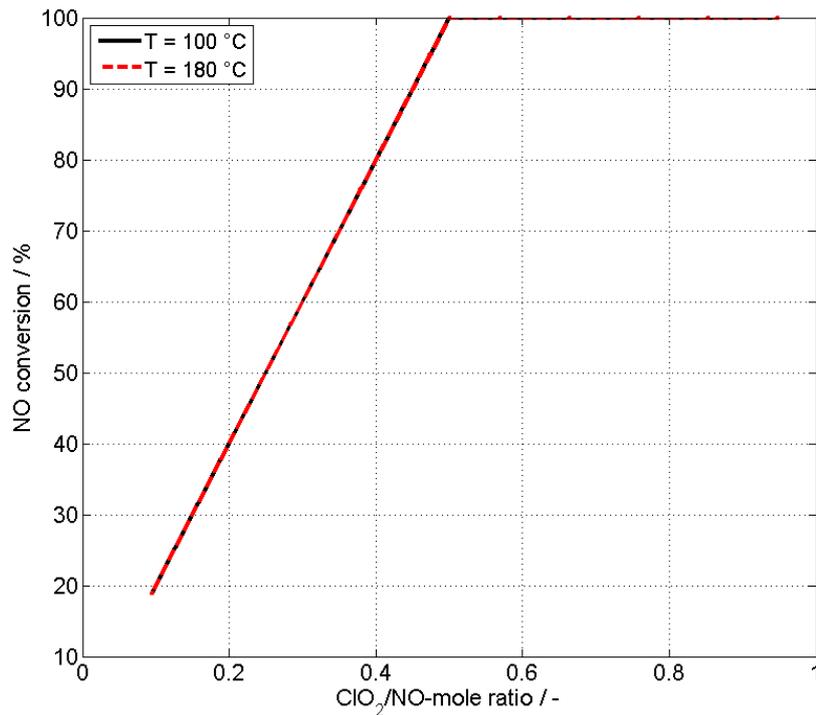
Figure 5.9: Effect of temperature on NO conversion.

Effect of temperature on SO_2 conversion: The activation Energy for $Cl + ClO_2 \longrightarrow 2\,ClO$ is negative and for $2\,ClO \longrightarrow Cl + ClO_2$ positive. A rising temperature induces therefore in a decreasing reaction kinetic for the first reaction

and an increasing one for the second. Thus higher temperatures in the reactor lead to a lower ClO presence in the reactor. For the SO_2 conversion the amount of ClO is important. A decreasing ClO amount induces in a lower SO_2 conversion, as illustrated in Figure 5.10.
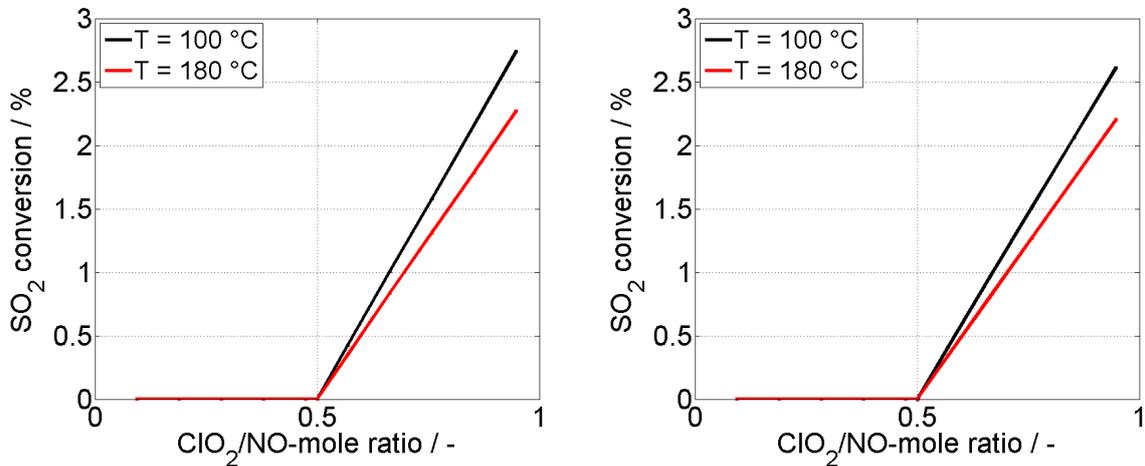
Figure 5.10: Effect of temperature on SO_2 conversion for 350 ppm SO_2 content (left) and 700 ppm SO_2 content (right).

Summary: NO conversion is not effected by residence times between 1.65 s – 3 s or reactor temperatures 100 °C – 180 °C. The SO_2 conversion is influenced, but only in a small range. As the solubility of sulfur dioxide is already higher than NO_2 no high value is set on converting this component much further, especially when it is linked to much higher costs. By increasing the residence time of 40% the reactor volume has to be increase about the same amount. This costs not only material but also area.

At a ClO_2/NO-ratio of 0.50 nearly 100% of the present NO is converted. Therefore and to keep the amount of used oxidizing agent down the ratio value is set to 0.50. Another point is, that the Cl compounds in the flue gas need to be kept down. For cleaning the flue gas these compounds have also to be washed out in the absorber, which leads to an higher amount of needed scrubbing water. To keep the used water low, the pollution of the flue gas has to be as low as possible.

By taking all results of the tested specifications and the the above mentioned fact into account the following is the best set up (of the tested conditions) for the reactor.

- Reactor residence time: 1.65 s

- Temperature: 100 °C

- ClO_2/NO-ratio: 0.50

6

Absorber performance

The different conditions for the absorption are summarized in Table 6.1. Each composition is tested with three different water amounts (further referred low, medium and high) and each of these with and without sodium hydroxide. The full experimental flue gas composition is additionally tested with realistic water amount of common SOx scrubbers as well as with HNO_2 in the scrubber water, so that it results in 30 different tested conditions. The results of those different absorption conditions are discussed in this chapter.

For the following figures the flue gas enters the absorber at Stage 1, which represents the bottom of the tower. The top of the absorber, where the gas leaves and the water enters the tower is Stage 50. All the reactions take part between the second and the 49th stage (first and last Stage excluded for the sake of simulation stability).

Table 6.1: Tested conditions for the absorption.

Flue gas composition	Liquid to gas ratio $l\ m^{-3}$	NaOH to liquid ratio -
S-compounds only	3.6/5.2/9.5	0/0.025
N-compounds only	3.6/5.2/9.5	0/0.025
NOx and SOx	3.6/5.2/9.5	0/0.025
Experimental composition	0.5/3.6/5.2/9.5	0/0.025//250[1]

1): HNO_2 flow in kg hr^{-1}

Effect of water amount on NO_2 and N_2O_4 absorption: The absorption of NO_2 is neither influenced by the pH-value nor by the presence of other pollutants, because it is a kinetic reaction and thus only influenced by the concentration of dissolved NO_2. The amount of water has an effect because the change in the relative amount of dissolved NO_2 (more water for the same amount of NO_2) causes a faster absorption of the NO_2. This effect can be seen in Figure 6.1. It also shows that N_2O_4 is not influenced by the water amount because its absorption takes place so fast that after a few stages no considerable amount is left in the gas phase.

That leads to the conclusion that the reaction kinetics (Reactions 3.26 and 3.28) and the solubility (regarding the phase equilibrium of NO_2, not the velocity of the mass-transfer between the phases) are the limiting factors. Only very little NO_2 is in the liquid phase due to solubility so the water can only absorb more NO_2 when the dissolved NO_2 reacts to other products.
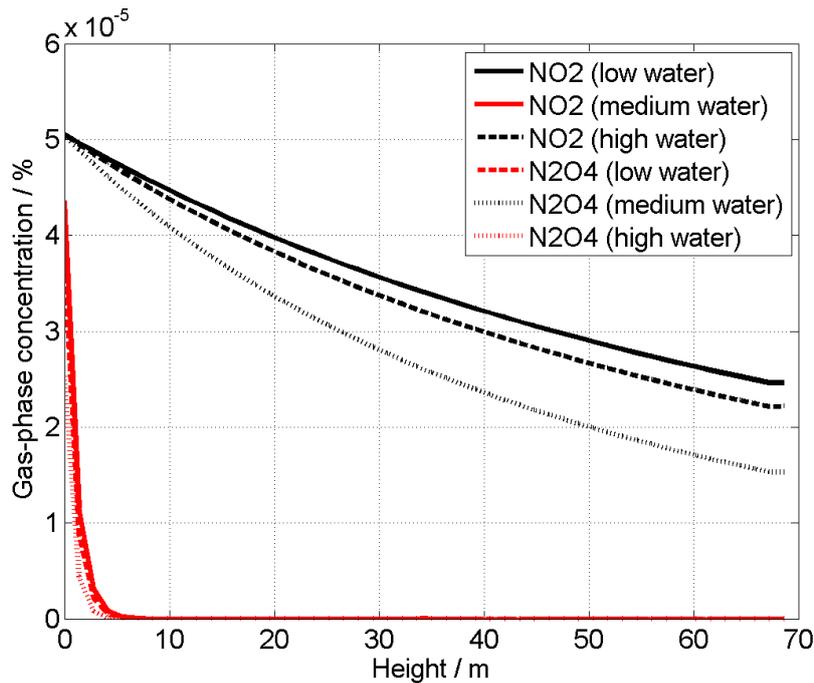
Figure 6.1: Dependency of NO2 content in vapor fraction by different amounts of used water.

Effect of pH-value on SO_2 absorption:SO_2 is very dependent on the pH-value and due to that, to other pollutants which effect the pH. The pH-value gets low by using only few water or by absorbing pollutants which lead to an decreasing pH. Then the SO_2 conversion starts not until the top of the absorber, where the pH-value is higher. After it is absorbed gas-phase and aqueous SO_2, as well as aqueous SO_2 and HSO_3^- are at equilibrium (visualized in Figure 6.2). If the pH-value in the scrubbing water is lower than one almost no SO_2 is dissolved because the dissolved SO_2 can not ionize to HSO_3^-.

For higher pH-values, because of NaOH in the scrubbing water or of a higher amount of water (same start pH-value but slower decline) the SO_2 is completely dissolved at the bottom stages of the absorber. Figure 6.3 shows the SO-compounds in the liquid-phase for the absorption with low water amount with and without NaOH. It also shows that more HSO_3^- can be present for the same amount of dissolved SO_2 because of the lower H^+-concentration.

Effect of the height on the absorption of SO_2 and NO_2: Figure 6.4 shows the effect of the absorber tower height on SO_2 and NO_2 absorption (the number of stages stays constant). The absorbent is pure water. The gas cleaning efficiency for SO_2 stays, in spite of the radical change in height, nearly constant. This leads to the conclusion that the height (between 7 and 70 m) has not much influence on the over all SO_2 absorption. It is assumed that the change in course of the curve is due to the higher resolution (one stage per 0.14 m instead of 1.4 m) and that the constant equilibrium state in the middle is taken out. With further height reduction the SO_2 absorption efficiency gets worse more rapidly. The NO_2 on the other hand is way
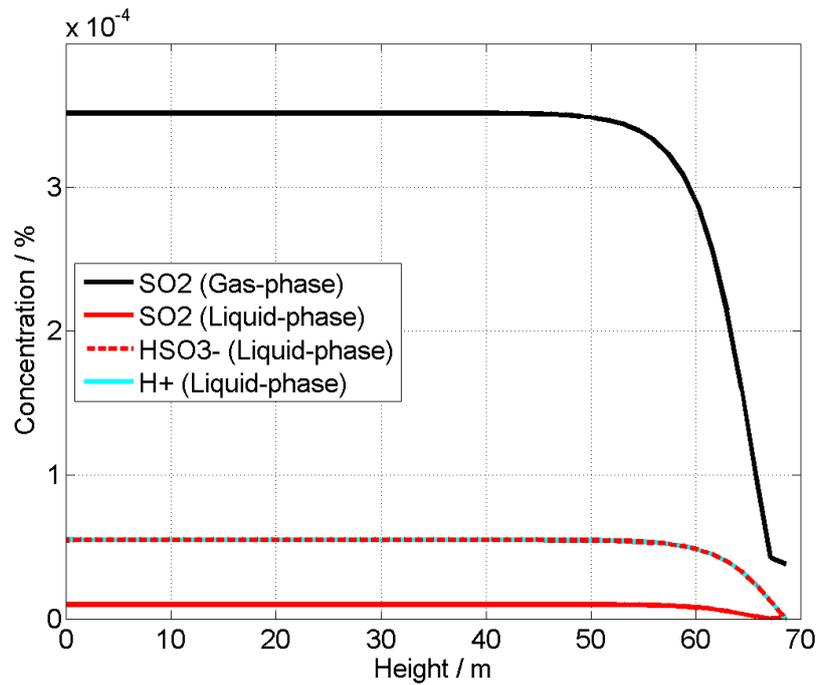
Figure 6.2: Equilibrium between gaseous and aqueous SO_2 as well as between aqueous SO_2 and sulfurous acid.
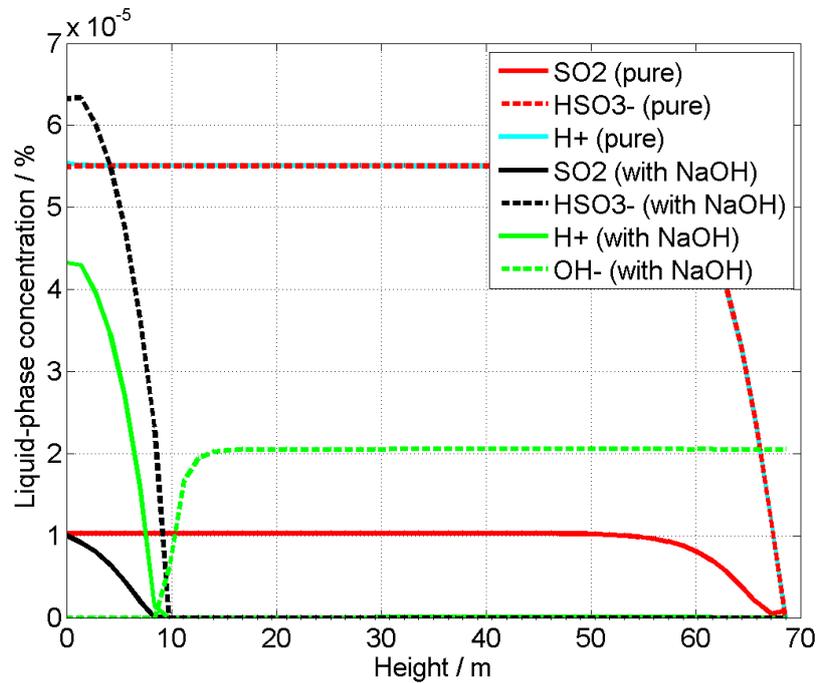
Figure 6.3: Dependency of the equilibrium between aqueous SO_2 and sulfurous acid of the pH-value (H^+ concentration).

less efficiently absorbed due to height reduction. This is not problematic in our case because the NO_x emission limit is reached even with nearly no absorption, therefore

the lower height is sufficient.
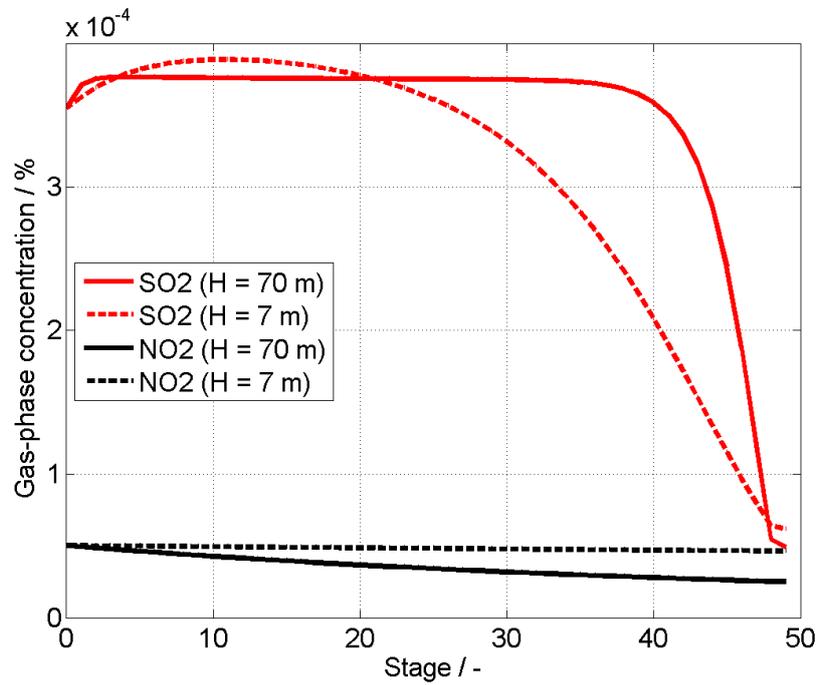
Figure 6.4: Dependency of SO_2 and NO_2 of the height of the absorber.

Effect of different absorbents (NaOH and HNO$_2$) on the absorption of SO$_2$ NO$_2$ and HNO$_2$: To increase the efficiency different absorbents are tested. In a first try NaOH is added while allowing only the water equilibrium reaction to only see the impact of the pH value. Secondly HNO$_2$ is added to see the influence of the interaction reactions. Neither the NO$_2$ nor its reaction products are effected by the pH-value. Low pH-value causes the HNO$_2$ equilibrium reaction (compare Reaction 3.31) to be on the left so that a considerable amount of HNO$_2$ is present in the gas- as well as the liquid-phase. Because the pH value is without NaOH (average pH = 2.7) and with NaOH (average pH = 4.0) still below the value where HNO$_2$ could dissociate, the HNO$_2$ absorption is not influenced by adding sodium hydroxide in the tested amounts. At higher pH-values HNO$_2$ would mostly be ionized to NO$_2^-$ which is then present only in liquid-phase, but such high pH values are not reached in the absorber. The SO$_2$ is contrary to the N-compounds strongly influenced by the pH value. This is as described in Figure 6.3 because of the HSO$_3^-$ aqueous SO$_2$ equilibrium, and that effects the absorption because the dissociation of H$_2$SO$_3$ takes place in the pH range present in the absorber. Beside the pH influence Figure 6.5 also shows the influence of the interaction reactions. With the HNO$_2$ in the absorber water the interaction reactions can take place over the whole height of the absorber. The advantage of that is that the SO$_2$ absorption is far more efficient, the disadvantage is that more HNO$_2$ and N$_2$O is present in the flue gas. A solution for that could be to combine pH control and HNO$_2$ in the feed stream. That would lead to an enlargement of the interaction reactions while keeping the pH value high enough so that mainly the interaction reaction building HADS would take place. Additionally the HNO$_2$ could be fed in a lower stage so that it can be absorbed in the top stages and would not be present in the exiting gas stream.
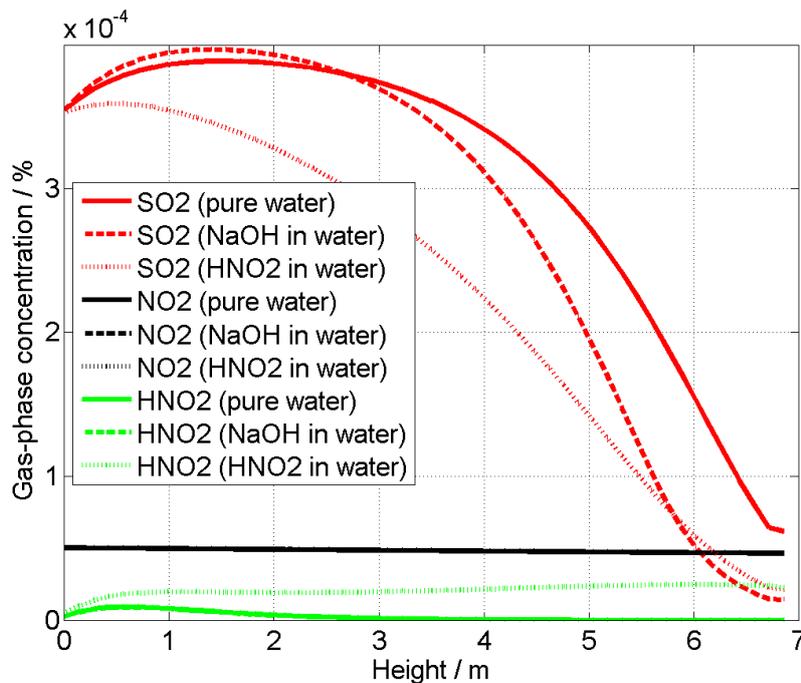
Figure 6.5: Dependency of SO$_2$ NO$_2$ and HNO$_2$ of the absorbents.

Effect of HNO$_2$ in scrubbing water on interaction reaction products: The reactions to form HADS and N$_2$O take place equally. So as Figure 6.6 shows, the produced mole-fraction of HADS and the sum of HSO$_4^-$ and SO$_4^{2-}$ are equal. The N$_2$O fraction referred to the water stream is half the fraction of HADS. As mentioned in the paragraph before the addition of HNO$_2$ to the water stream leads to more interaction reaction. As mentioned in 2.3.2 the N$_2$O formation is not favourable, a solution to combine the positive effect of the interaction reaction while avoiding the N$_2$O formation could be the combination of HNO$_2$ in the scrubbing water and pH control by adding NaOH to keep the pH value around 4, so that only the interaction reaction forming HADS would take place.
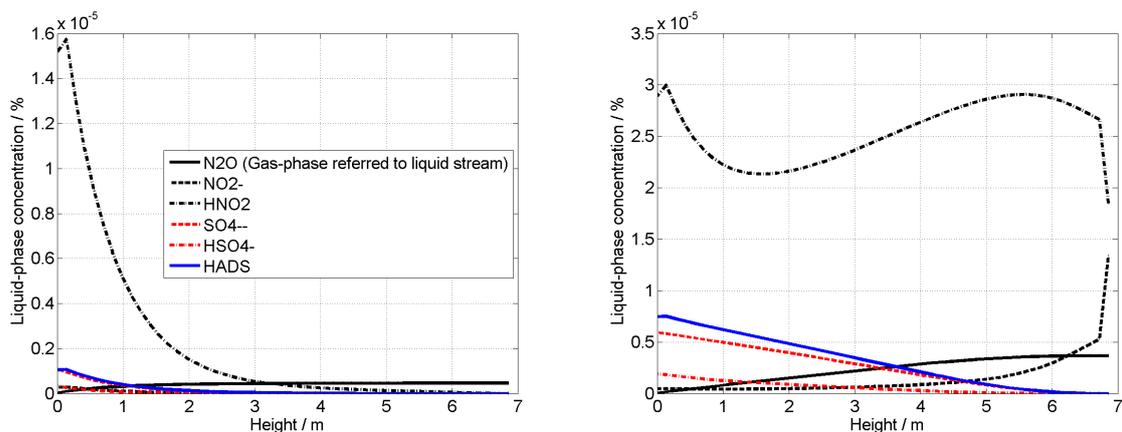
Figure 6.6: Interaction products for pure water (left) and for HNO$_2$ Solution (right) (legend suits for both graphs).

Effect of water flow on the absorption of chlorine compounds: For the reason that the water amount is not comparable to usual absorbers, the simulation was again run for the liquid to gas ratio of 0.5 which is the maximum for usual packed bed towers. The Cl$_2$ as well as the Cl contents in the flue gas are low and therefore also fast absorbed for low pH-values and few water (less water leads to a lower pH-value). This is illustrated in Figure 6.7, whereas a low L/G-ratio also represents lower pH-values. Theoretically the Cl$_2$ absorption is strongly pH dependent too (same as SO$_2$ absorption) but due to HCl is a much stronger acid than H$_2$SO$_3$ the effect would get visible at much lower pH-values which are not reached in this case. The ClO absorption is more problematic because it just dissolves without further reacting (no reaction could be found in literature), so the lower water amount leads to the worse absorption. But its vapor fraction is low enough that even with the water amount of common scrubbers the emission limit is reached.
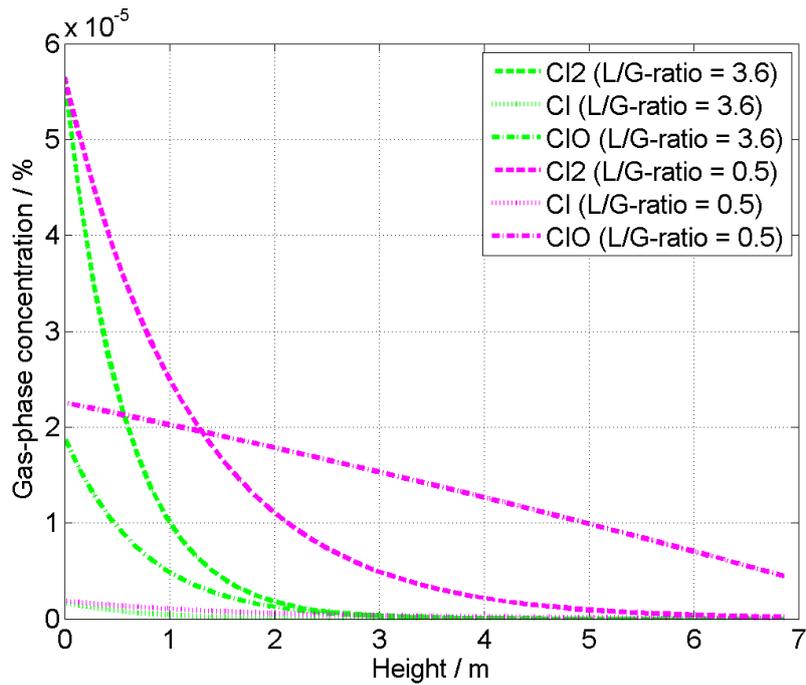
Figure 6.7: Absorption of chlorine compounds.

As can be seen in Figures 6.8 and 6.9 the N_2O_4 is still fast absorbed whereas the NO_2 fraction is only a little reduced. Therefore the resulting efficiencies for NO_x (58.17%) and SO_x (16.24%) are quite low compared to commercial desulfurisation and reduction measures. The scrubbing efficiency for Cl-compounds with 94.49% is in the range of usual packed bed absorbers (compare Table 4.7 in Chapter 4.2). By that it can be seen that the usual amount of water is not sufficient for this application. The resulting composition curves in the gas and the liquid phase are shown in Figure 6.8 and 6.9 respectively.
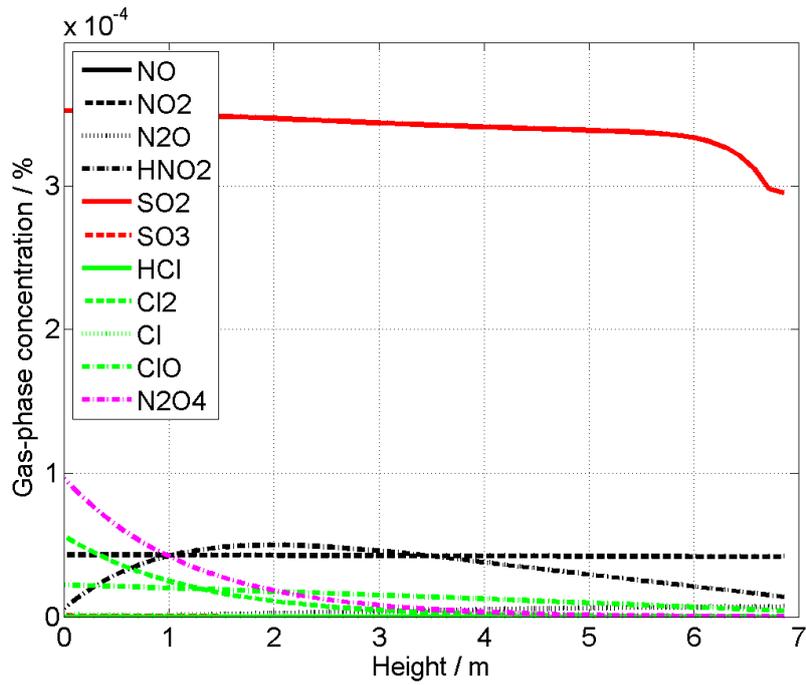
Figure 6.8: Vapor composition of experimental flue gas absorption with realistic water amount.
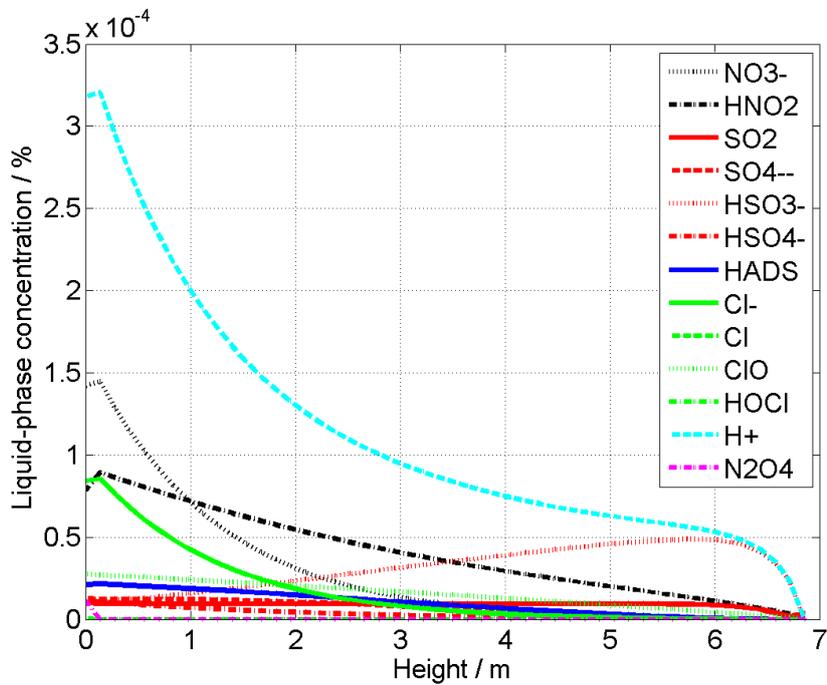
Figure 6.9: Liquid composition of experimental flue gas absorption with realistic water amount.

7

System performance

After the separate consideration of the reactor and the absorber the complete system is evaluated in this chapter. The obtained results of the whole system model are presented. To achieve knowledge about the cleaning efficiency of the NO_x removal concept it is tested for the flue gas composition of a coal power plant (Table 7.1 Point 1). For the absorber two different scrubbing solutions are verified. The first one is pure water, while the second one consists of Water, NaOH and HNO_2. As mentioned before in chapter 6 NaOH is needed to change the pH-value. For desulfurization plants with lime slurry the pH is around 12.5. The amount of HNO_2 is with 250 kg hr^{-1} the same as during the trails for the absorber. For both two different set ups are used:

- The first one is to use as much water as needed to achieve the NO_x and SO_x emission limits of a 300 MW coal power plant (NO_x: 150 ppm; SO_x: 150 ppm).

- The second set up is using the common desulfurization liquid to gas ratio for wet scrubbers (L/G-ratio: 0.5 l m^{-3}).

Furthermore all simulations use a ClO_2/NO-ratio of 0.50. At this ratio former reactor simulations showed the first time complete NO conversion. Therefore 0.50 ClO_2/NO-ratio is used to keep the chlorine amount inside the system as low as possible and still achieve full NO conversion in the reactor. The other set up of the reactor is already given in the result summary of the reactor simulation.
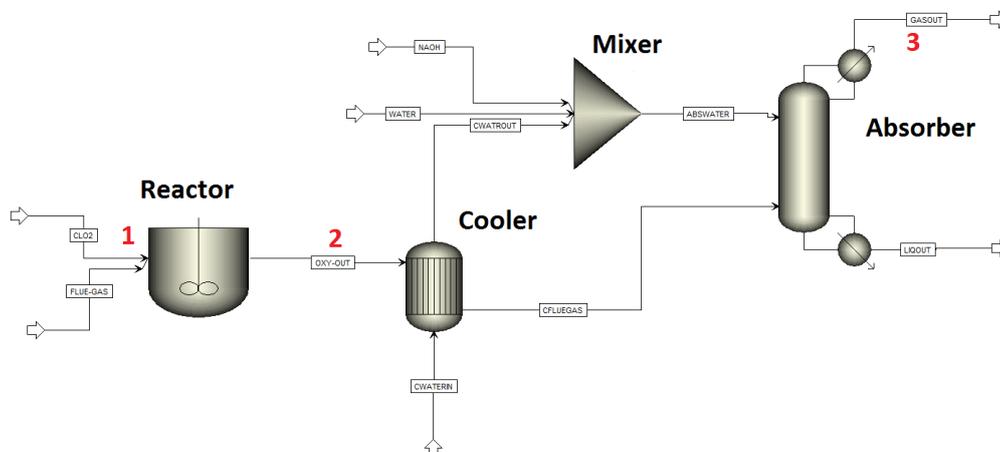
Figure 7.1: Flowsheet of the NO_x removal simulation model.

Figure 7.1 illustrates the flowsheet of the simulation model. The mixer is used to merge the water streams for the absorber. One comes from the cooler, where it is used to cool the flue gas after the reactor. The second water stream is a variable one where the amount of used water in the absorber can be controlled. The last stream which goes into the mixer is the NaOH one for the pH control.

The flue gas compositions at three different points are given in Table 7.1. These points are also illustrated in Figure 7.1 (red numbers). 3.1 are the results for the absorber driven with pure water and 3.2 the results for the scrubbing solution with NaOH and HNO_2. The composition plots for each phase, gas and liquid, are given in Appendix B.

Table 7.1: Flue gas compositions at the three measuring points.

compound	mole-fraction					
	1	**2**	**3.1.1** [1]	**3.1.2** [2]	**3.2.1** [1]	**3.2.2** [2]
N_2 / %	70.33	70.33	72.58	72.51	72.53	72.46
CO_2 / %	20.80	20.80	21.33	21.43	21.34	21.42
O_2 / %	3.40	3.40	3.51	3.51	3.51	3.50
H_2O / %	5.30	5.30	2.57	2.42	2.61	2.51
SO_2 / ppm	1,343	1,344	55.16	1,235	55.00	965
SO_3 / ppm	0	0.10	0	0	0	0
NO / ppm	331	1.00	1.00	1.00	1.00	1.0
NO_2 / ppm	56.4	63.56	58.30	62.77	58.96	62.95
N_2O_4 / ppm	0	161.5	0	0.50	0	0.50
HNO_2 / ppm	0	0	0.03	12.92	0	7.56
N_2O / ppm	0	0	4.46	16.64	29.42	55.40
Cl / ppm	0	3.40	0	0.09	0	0.09
Cl_2 / ppm	0	80.70	0	0.34	0	0.30
ClO / ppm	0	0.80	0	0.14	0	0.14
ClO_2 / ppm	0	0.03	0.03	0.03	0.03	0.03
Water amount / kg hr^{-1}			6,908,590	505,723	5,662,360	505,723

[1]: flue gas composition with solution amount to achieve emission limits

[2]: flue gas composition with solution amount of common wet scrubbers

For both scrubbing solutions and set ups a NO conversion of over 99%, after the reactor is possible. Also most of the nitrogen is present as N_2O_4 in the flue gas. That leads to a better solubility of the N-pollutions, because of the higher solubility of N_2O_4 compared to NO_2.

Pure water as scrubbing solution

Emission limits set up: Point 3.1.1 in Table 7.1 represents the results with meeting the emission limits for the pure water solution. It can be seen that there is still NO_2 present in the cleaned flue gas. This is a total amount of 15.04% and the whole

N_2O_4 is removed. Therefore the cleaning efficiency for NO_x in that case is 84.87%. Also the cleaning efficiency for SO_x is with 95.89% high. With this set up it is also possible to remove 99.98% of Cl compounds from the flue gas.

L/G-ratio set up: The results for this set up are presented under point 3.1.2. There is still NO_2 and N_2O_4 present in the cleaned gas. A cleaning efficiency for NO_x of 80.20% is achieved. The water amount is too low for high SO_x removal. Only a efficiency of 8.04% is reached. With this set up also nearly all Cl compounds (99.51%) are removed.

Water, NaOH and HNO$_2$ as scrubbing solution

Emission limits set up: Point 3.2.1 in Table 7.1 represents the results with meeting the emission limits for the modified scrubbing solution. It can be seen that there is still NO_2 present in the cleaned flue gas, which is slightly higher than the NO_2 output by using pure water in the scrubber. Reason for this is the of 18% reduced amount of scrubbing solution needed to reach the emission limits compared to the pure water option. Therefore the cleaning efficiency for NO_x in that case is 84.52%. Also the cleaning efficiency for SO_x is with 95.90% high. With this set up it is also possible to remove the whole Cl compounds from the flue gas.

L/G-ratio set up: The results for this set up are presented under point 3.2.2. There is also still NO_2, N_2O_4 and HNO_2 available in the cleaned gas. But although HNO_2 is added in the scrubbing water the amount in the exiting flue gas is lower. The reason for that is the better SO_2 absorption due to the higher pH-value and the higher resulting HSO_3^- in the liquid. Because of that more interaction reaction can take place by which the HNO_2 amount is reduced. At the same time the interaction reactions increase the N_2O amount which is not accounted for the NO_x emission. The cleaning efficiency for NO_x is with 81.28% high enough to achieve the emission limits. The water amount is too low for high SO_x removal. Only a efficiency of 28.15% is reached. With this set up also nearly all Cl compounds (99.48%) are removed.

To sum up it is possible to achieve the EU emission limits for CL-N-S compounds for coal power plants by using pure water as a scrubbing solution. The needed water amount is in that case more than 13 times higher than the L/G ratio for common wet scrubbers used for desulfurization. This has negative effect on the running costs as well as the dimensions of the absorber tower. Thus more research on the absorption has to be done. Especially for the absorbent, it is better to use some additives than pure water.
By adding pH control (NaOH) as well as HNO_2 in an amount that could come from a recycled stream to the scrubbing solution, it was possible to reduce the needed water amount of about 18%. By adding external HNO_2 the needed water flow could be further reduced. A critical value is then the NO_x emission limit, because if too much HNO_2 is added it is also present in the exhaust gas. The addition of HNO_2 to the scrubbing water has also a increasing effect on the N_2O generation. This could be avoided by keeping a constant pH-value (pH = 4) over the whole absorber. Thus the positive effect of the interaction reactions would be kept without emitting N_2O, which is a strong greenhouse gas.

8

Conclusion and Prospects

To limit the emission of harmful components like NO_x, SO_x and Cl-compounds, flue gas treatment processes are of major relevance. Those concepts are especially for power and waste incineration plants, since here a lot of emissions are present. Already existing and state of the art examples are SNCR, SCR for NO_x and wet scrubbers for SO_x removal. These measures are only constructed to remove one kind of pollution. Therefore one system for each pollution is needed, which leads to large investment and running cost.

A new concept is investigated, that allows a simultaneously removal of NO_x and SO_x and should therefore lead to a cost reduction.

The objective of this work was to evaluate the new NO_x and SO_x removal concept under conditions relevant to the flue gas output. This was done by modeling the system with ASPEN PLUS.

The procedure as well as the outcome are summarized in the following:

1. At the beginning the removal concept was separated into two parts, the reactor and absorber. For each system component the possible chemical reactions as well as their kinetics were considered.

2. Subsequently the reactor model was compared to the experiments. For this a synthetic flue gas was tested in a reactor test rig under different process conditions. A maximum accuracy of 10% for NO conversion could be achieved. Thus the reactor simulation model was declared as suitable for further simulations.

3. Also the simulation model of the absorber was tested and the results were considered for plausibility. Furthermore the influence of different absorption parameters (Liquid to gas ratio, pH-value and flue gas composition) was considered.

4. Afterwards both reactor and absorber were merged and the whole system was tested for the flue gas composition of a coal power plant. Two different set ups were analyzed and a maximum efficiency of 84.52% for NO_x and 95.90% for SO_x was achieved.

With regard to the complete evaluation of the new removal concept a some more observations are needed. Following points are important:

1. The needed water in the absorber has to be put to a minimum amount. Therefor more research on the absorbent has to be done. Additives for a better solubility and faster reaction of the pollutions with the washing water should be tested. Also a recycling concept for the waste water should be investigated.

2. Another model that should be tested, is to extend the existing model by an second absorber (Figure 8.1). This should be placed upstream the reactor to absorb the SO_2, before the flue gas is entering the reactor. By using the waste water of the downstream reactor (containing HNO_2) as the scrubbing water the absorption is enhanced due to the interaction reaction.

3. To find out if the NO_x and SO_x removal concept is cost efficient, a cost calculation should be done.

4. For studying the effect of different washing water conditions as well as to validate the absorber simulation model a wet scrubber should be implemented to the test rig.
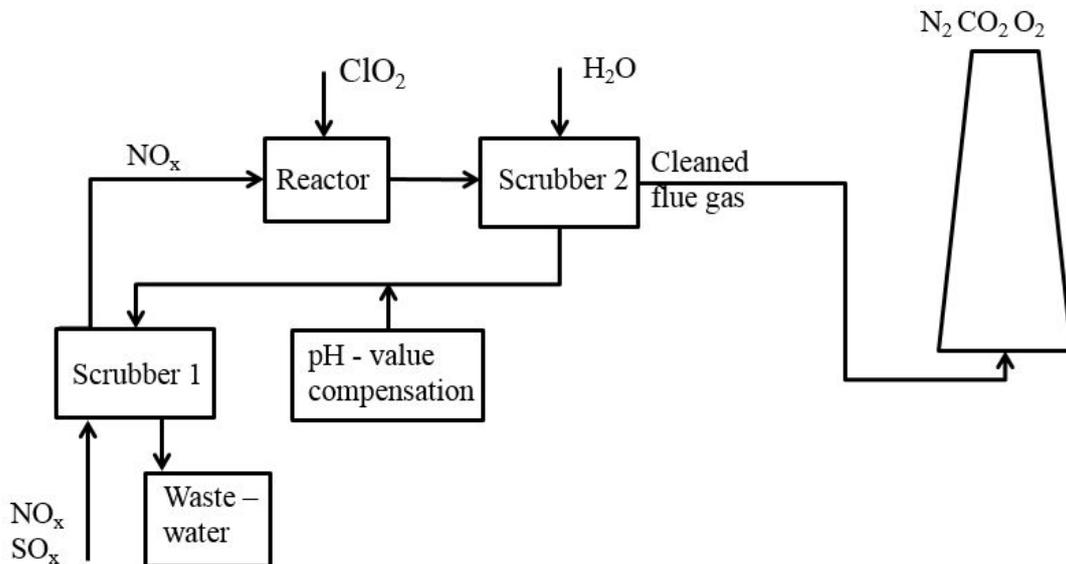
Figure 8.1: Flowsheet of the removal concept with two scrubbers.

Bibliography

[1] G. BAUMBACH, *Flue gas cleaning at combustion plants*, Lecture, 2013.

[2] F. POPESCU, I. IONEL, *Anthropogenic Air Pollution Sources*, http://www.intechopen.com/books/airquality/anthropogenic-air-pollution-sources visited: 2015-01-20.

[3] T. HAGN, *Linde technology #1.12*, Linde AG Munich, 2012.

[4] R. RITTER, T. STOFFREGEN, N. SCHÖDEL, F.WINKLER, *NO_X processing experiences for removal in the CO_2 plant in the Oxyfuel combustion process*, 3rd Oxyfuel Combustion Conference, 2013.

[5] S. AJDARI, F. NORMANN, K. ANDERSSON, F. JOHNSSON, *Gas phase oxidation of SO_2 by NO_2 in pressurized flue gas systems - an experimental investigation*, 3rd Oxyfuel Combustion Conference, 2013.

[6] S. AJDARI, F. NORMANN, K. ANDERSSON, *Control of NO_X and SO_X in Chemical – Looping Combustion Plants: The Importance of Pressurized Flue Gas Systems* , 3rd International Conference on Chemical Looping, 2014.

[7] R. ATKINSON, D. BAULCH, R. COX, J. CROWLEY, R. HAMPSON, R. HYNES, M. JENKIN, M. ROSSI, J. TROE, *Evaluated kinetic and photochemical data for atmospheric chemistry: Volume I-gas phase reactions of* O_x HO_x and SO_x *species*, Atmospheric chemistry and physics 4, 2004, 1461 – 1738.

[8] H. TSUKAHARA, T. ISHIDA, M. MAYUMI, *Gas-Phase oxidation of nitric oxide: Chemical kinetics and rate constant* , Nitric oxide - biology and chemistry 3, 1999, 191 – 198.

[9] R. ATKINSON, D. BAULCH, R. COX, J. CROWLEY, R. HAMPSON, R. HYNES, M. JENKIN, M. ROSSI, J. TROE, *Evaluated kinetic and photochemical data for atmospheric chemistry: Volume III-gas phase reactions of inorganic halogens*, Atmospheric chemistry and physics, 2006.

[10] R. GRIFFIN, *Principles of Air Quality Management, Second Edition*, Taylor & Francis Group, 2006, 176 – 177.

[11] G. BAUMBACH, *Air quality control*, Springer, 1996, 397 – 417.

[12] P. ROBERTS, L. WHITE, *Cost effectiveness of emissions abatement option in European refineries*, concawe air quality management, CONCAWE, Brusssels, 2011.

[13] S. KISAMORI, S. KAWANO, I. MOCHIDA, SO_2 *AND* NO_x *removal at ambient temperatures using activated carbon fibers*, Institute of Advanced Material Study in Kasuga, Japan, 1993.

[14] S.G. CHANG, D. LITTLEJOHN N.H. LIN, *Kinetics of Reactions in a Wet Flue Gas Desulfurization and Denitrification System*, American Chemical Society, 1982.

[15] M.T. LEU, W.B. DEMORE, *Rate constant for the reaction* $ClO + NO \longrightarrow Cl + NO_2$, Journal of Physical chemistry Vol. 82 No. 19, 1978.

[16] Z. LI, R.D. WUEBBLES, N.J. PYLAWKA, *Rate constant measurement for the reaction of OClO with NO at 220-367 K*, Chemical Physical Letters 354, 2002, 491 – 497.

[17] C. ENGLAND, W.H. CORCORAN, *The rate and mechanism of the air oxidation of parts-per-million concentrations of nitric oxide in the presence of water vapor*, Industrial and Engineering chemistry fundamentals, 1975, 55 – 63.

[18] Z.D. XIE, *Formation mechanism of condensation nuclei in nighttime atmosphere and the kinetics of the SO2-O3-NO2 system*, Journal physical chemistry, Vol. 96, 1992, 1543 – 1547.

[19] R.E. EIBLING, M. KAUFMAN, Atmospheric Environment, 17, 1983, 429 – 431.

[20]] M.G. BRYUKOV, B. DELLINGER, V.D KNYAZEV, *Kinetics of the gas-phase reaction of OH with HCl*, Journal physical chemistry, Vol. 110, 2006, 936-943.

[21] R.P. WIDMAN, B.A. DEGRAFF, *On the gas-phase recombination of chlorine atoms*, Journal physical chemistry, Vol.77, 1973, 1325-1328.

[22] J. W. ARMITAGE, C.F. CULLIS, *Studies of the Reaction between Nitrogen Dioxide and Sulfur Dioxide*, Combustion and Flame, Vol.16, 1971.

[23] T. HIGASHIHARA, K. SAITO, I. MURAKAMI, *The reaction of hydrogen chloride with nitrogen oxide in shock waves*, Bulletin of the Chemical Society of Japan, Vol. 51, 1978.

[24] G. POULET, G. LEBRAS, J. COMBOURIEU, *Kinetic study of the reactions of Cl atoms with HNO3, H2O2, and HO2*, Journal of chemical physics, Vol. 69, 1978.

[25] P. BORRELL, C.J. COBOS, K. LUTHER, *Falloff curve and specific rate constants for the reaction NO2 + NO2 N2O4*, Journal physical chemistry, Vol. 92, 1988., 4377 – 4384.

[26] R. Atkinson, D. Baulch, R. Cox, R.F. Hampson, J.A. Kerr, M.J. Rossi, J. Troe, *Evaluated kinetic and photochemical data for atmospheric chemistry: supplement VI. IUPAC subcommittee on gas kinetic data evaluation for atmospheric chemistry*, Journal physical and chemical reference data, Vol. 26, 1997, 1329 – 1499.

[27] L.C. Anderson, D.W. Fahey, *Studies with ClONO2: Thermal dissociation rate and catalytic conversion to NO using an NO/O3 chemiluminescence detector*, Journal of physical chemistry, Vol. 94, 1990, 644 – 652.

[28] W.A. Rosser, H. Wise, *Kinetics of the gas phase oxidation of hydrogen chloride and of hydrogen bromide by nitrogen dioxide*, Journal of physical chemistry, Vol. 64, 1960, 602 – 604.

[29] J. A. Coxon, *Reaction between Chlorine Dioxide and Nitric Oxide*, Queen Mary College in London, England, 1968.

[30] B. R. Deshwal, D. S. Jin, S. H. Lee, S. H. Moon, J. H. Jung, H. K. Lee, *Removal of NO from flue gas by aqueous chlorine-dioxide scrubbing solution in a lab-scale bubbling reactor*, Journal of Hazardous Materials 150, 2008, 649 – 655.

[31] J. J. Kaczur, *Oxidation chemistry of chloric acid in NOx/SOx and air toxic metal removal from gas streams*, Environmental Progress Vol. 15, No. 4, 1996.

[32] B. R. Deshwal, D. S. Jin, Y. S. Park, H. K. Lee, *Simultaneous removal of SO_2 and NO by wet scrubbing using aqueous chlorine dioxide solution*, Journal of Hazardous Materials B135, 2006, 412 – 417.

[33] J. Mizeraczyk, M. Dors, *Direct and indirect ozone methods for NO_X removal*, Szewalski Institute of Fluid Flow Machinery, Fiszera, Poland, 2010.

[34] E. S. Tavoulares, W. Joyewicz, *Multipollutant Emission Control Technology Optionsfor Coal-fired Power Plants* , U.S. Environmental Protection Agency, USA, 2005.

[35] European Commission, *Best available techniques for large combustion plants*, Integrated Pollution Prevention and Control, European Union, 2006.

[36] European Union, *Directive 2010/75/EU of the European Parliament and of the Council on industrial emissions*, Official Journal of the European Union, 2010, pp. 62 – 65.

[37] R. Schefflan, *Teach yourself the basics of Aspen Plus*, John Wiley & Sons, 2011.

[38] M. A. Siddiqi, J. Petersen, K. Lucas, *A Study of the Effect of Nitrogen Dioxide on the Absorption of Sulfur Dioxide in Wet Flue Gas Cleaning Processes*, Industrial & Engineering Chemistry Research 40, 2116 – 2127, 2001.

[39] M. Pires, M. Rossi, *The Heterogeneous Formation of N2O in the Presence of Acidic Solutions: Experiments and Modeling*, Ecole Polytechnique Fédérale de Lausanne (EPFL), Switzerland, 1997.

[40] K. Omar, *Evaluation of BOC's* LoTOx^{TM} *process for the oxidation of elemental mercury in flue gas from a coal-fired boiler*, Western Research Institute, Wyoming, 2008.

[41] Testo, *Testo 350 Emission Analyzer*,
http://www.testo350.com/testo-350/350anadefsx/350faqs.html visited: 2015-03-19.

[42] *Flue gas analysis in industry*,
http : //www.testo350.com/downloads/Flue$_G$as$_i$n$_I$ndustry$_0$981$_2$773.pdf visited: 2015-04-24.

[43] Bronkhorst, *Thermal mass flow measurement*,
http : //www.bronkhorst.com/en/products/theory/thermal$_m$ass$_f$low$_m$easurement/ visited: 2015-03-19.

[44] R. E. Dickerson, H. B. Gray, G. P. Haight, *Chemical Principles, Third Edition, Chapter 5: Solution Equilibria: Acids and Bases*, pp. 172 – 225, 1979.

[45] D. Wu, D. Wong, B. Di Bartolo, *Evolution of Cl2- in aqueous NaCl solutions*, Journal of Photochemistry, 14 , pp. 303 – 310, 1980.

[46] Y.-N. Lee, S. E. Schwartz, *Reaction Kinetics of Nitrogen Dioxide with Liquid Water at Low Partial Pressure*, Journal of Physical Chemistry, 85, pp. 840 – 848, 1981.

[47] S. P. Tan, M. Piri, *Modeling the Solubility of Nitrogen Dioxide in Water Using Perturbed-Chain Statistical Associating Fluid Theory*, Department of Chemical and Petroleum Engineering, University of Wyoming, United States, 2013.

[48] J.-Y. Park, Y.-N. Lee, *Solubility and Decomposition Kinetics of Nitrous Acid in Aqueous Solution*, Journal of Physical Chemistry, 92, pp. 6294 – 6302, 1988.

[49] K. D. Fogelmann, D. M. Walker, D. W. Margerum, *Non-Metal Redox Kinetics: Hypochlorite and Hypochlorous Acid Reactions with Sulfite*, Inorganic Chemistry, 28, pp. 986 – 993, 1989.

[50] W. Barbour, R. Oommen, G. S. Shareef, W. M. Vatavuk *EPA Air Pollution Control Cost Manual, Section 5: SO2 and Acid Gas Controls*, Research Triangle Park, 1995.

[51] W.K. Lewis, W.G. Whitman *Principles of Gas Transfer Absorption*, Industrial and Engineering Chemistry, Vol. 16, No. 12, pp. 1215-1237, 1924.

[52] A. A. Keller, *Rate-Limited Mass Transfer Between Phases*, School of Environmental Science & Management, 2013.

[53] M. K. STENSTROM, *Gas Transfer*, Civil and Environmental Engineering Department,
http : //www.seas.ucla.edu/stenstro/ visited: 2015-04-17.

[54] D. D. EBBING, *General Chemistry 3rd ed.*, Houghton Mifflin Company: Boston, pp 217, 303, 1990. http : //chemistry − reference.com/reaction.asp?rxnnum = 590 visited: 2015-04-12.

[55] B. K. SCHNELLE, C. A. BROWN, *Air pollution control technology handbook*, CRC Press, 2001.

[56] WET SCRUBBERS, http://www.epa.state.oh.us/portals/27/engineer/eguides/scrubbers.pdf visited: 2015-04-20.

[57] PH. MOISY, I. BISEL, F. GENVO, F. REY-GAUREZ, L. VENAULT, P. BLANC, *Preliminary results on the effect of power ultrasound on nitrogen oxide and dioxide atmosphere in nitric acid solutions*, Ultrasonics Sonochemistry 8, pp. 175 − 181, 2001.

[58] J. R. FAIR, D. E. STEINMEYER, W. R. PENNY, B. B. CROCKER*Perry's Chemical Engineers' Handbook*, Seventh Edition, Section 14, pp. 1351 − 1449, 1197.

[59] R. L. SHILLING, K. J. BELL, P. M. BERNHAGEN, T. M. FLYNN, V. M. GOLDSCHMIDT, P. S. HRNJAK, F. C. STANDIFORD, K. D. TIMMERHAUS*Perry's Chemical Engineers' Handbook*, Seventh Edition, Section 11, pp. 1035 − 1152, 1197.

[60] ASPEN TECHNOLOGY INC., Aspen PLUS V8.2 (28.0.25), 2013.

Bibliography

A

Experiment and simulation results

In Tables A.1 and A.2 the RCSTR and REquil simulation results are listed.

Table A.1: Results of RCSTR-model simulations.

NO	SO$_2$	T	t$_{reaction}$	Water content	ClO$_2$/NO	NO conversion	SO$_2$ reduction
ppm	ppm	°C	s	vol.%	-	-	-
250	0	100	1.65	0	0.09	0.189	
					0.19	0.379	
					0.28	0.569	
					0.38	0.758	
					0.47	0.947	
					0.57	1.000	
					0.66	1.000	
250	350	100	1.65	0	0.09	0.190	0.000
					0.19	0.379	0.000
					0.28	0.569	0.000
					0.38	0.758	0.000
					0.47	0.948	0.000
					0.57	1.000	0.004
					0.66	1.000	0.010
					0.76	1.000	0.016
250	700	100	1.65	0	0.09	0.190	0.000
					0.19	0.379	0.000
					0.28	0.569	0.000
					0.38	0.759	0.000
					0.47	0.948	0.000
					0.57	1.000	0.004
					0.66	1.000	0.010
					0.76	1.000	0.015
					0.85	1.000	0.021
500	0	100	1.65	0	0.05	0.095	
					0.15	0.295	
					0.25	0.495	
					0.35	0.695	
					0.45	0.895	
					0.55	1.000	

					0.65	1.000	
					0.75	1.000	
					0.85	1.000	
					0.95	1.000	
500	350	100	1.65	0	0.05	0.095	0.000
					0.15	0.295	0.000
					0.25	0.495	0.000
					0.35	0.695	0.000
					0.45	0.895	0.000
					0.55	1.000	0.006
					0.65	1.000	0.018
					0.75	1.000	0.029
					0.85	1.000	0.040
					0.95	1.000	0.050
500	700	100	1.65	0	0.05	0.095	0.000
					0.15	0.295	0.000
					0.25	0.495	0.000
					0.35	0.695	0.000
					0.45	0.896	0.000
					0.55	1.000	0.006
					0.65	1.000	0.017
					0.75	1.000	0.028
					0.85	1.000	0.038
					0.95	1.000	0.048
250	0	100	2.3	0	0.09	0.190	
					0.19	0.379	
					0.28	0.569	
					0.38	0.758	
					0.47	0.947	
					0.57	1.000	
					0.66	1.000	
					0.76	1.000	
					0.85	1.000	
					0.95	1.000	
250	350	100	2.3	0	0.09	0.190	0.000
					0.24	0.485	0.000
					0.39	0.779	0.000
					0.54	1.000	0.003
					0.68	1.000	0.015
					0.83	1.000	0.028
					0.98	1.000	0.039
					1.13	1.000	0.042
					1.27	1.000	0.042
					1.42	1.000	0.046
250	700	100	2.3	0	0.09	0.190	0.000
					0.24	0.485	0.000

II

					0.39	0.780	0.000
					0.54	1.000	0.003
					0.68	1.000	0.015
					0.83	1.000	0.026
					0.98	1.000	0.037
					1.13	1.000	0.048
					1.28	1.000	0.048
					1.42	1.000	0.048
500	0	100	2.3	0	0.05	0.095	
					0.15	0.295	
					0.25	0.495	
					0.35	0.695	
					0.45	0.895	
					0.55	1.000	
					0.65	1.000	
					0.75	1.000	
					0.85	1.000	
					0.95	1.000	
500	350	100	2.3	0	0.05	0.095	0.000
					0.15	0.295	0.000
					0.25	0.495	0.000
					0.35	0.695	0.000
					0.45	0.895	0.000
					0.55	1.000	0.008
					0.65	1.000	0.024
					0.75	1.000	0.040
					0.85	1.000	0.054
					0.95	1.000	0.066
500	700	100	2.3	0	0.05	0.095	0.000
					0.15	0.295	0.000
					0.25	0.495	0.000
					0.35	0.695	0.000
					0.45	0.896	0.000
					0.55	1.000	0.008
					0.65	1.000	0.023
					0.75	1.000	0.038
					0.85	1.000	0.051
					0.95	1.000	0.064
250	0	180	1.65	0	0.09	0.190	
					0.19	0.379	
					0.28	0.569	
					0.38	0.758	
					0.47	0.947	
					0.57	1.000	
					0.66	1.000	
					0.76	1.000	

					0.85	1.000	
					0.95	1.000	
250	350	180	1.65	0	0.09	0.190	0.000
					0.19	0.379	0.000
					0.28	0.569	0.000
					0.38	0.758	0.000
					0.47	0.948	0.000
					0.57	1.000	0.004
					0.66	1.000	0.008
					0.76	1.000	0.013
					0.85	1.000	0.017
					0.95	1.000	0.021
250	700	180	1.65	0	0.09	0.190	0.000
					0.19	0.379	0.000
					0.28	0.569	0.000
					0.38	0.759	0.000
					0.47	0.948	0.000
					0.57	1.000	0.003
					0.66	1.000	0.008
					0.76	1.000	0.012
					0.85	1.000	0.017
					0.95	1.000	0.021
250	0	180	2.3	0	0.09	0.190	
					0.19	0.379	
					0.28	0.569	
					0.38	0.758	
					0.47	0.947	
					0.57	1.000	
					0.66	1.000	
					0.76	1.000	
					0.85	1.000	
					0.95	1.000	
250	350	180	2.3	0	0.09	0.190	0.000
					0.19	0.379	0.000
					0.28	0.569	0.000
					0.38	0.758	0.000
					0.47	0.948	0.000
					0.57	1.000	0.005
					0.66	1.000	0.011
					0.76	1.000	0.017
					0.85	1.000	0.023
					0.95	1.000	0.029
250	700	180	2.3	0	0.09	0.190	0.000
					0.19	0.379	0.000
					0.28	0.569	0.000
					0.38	0.759	0.000

					0.47	0.948	0.000
					0.57	1.000	0.005
					0.66	1.000	0.011
					0.76	1.000	0.017
					0.85	1.000	0.022
					0.95	1.000	0.028
250	0	100	3	0	0.09	0.190	
					0.19	0.379	
					0.28	0.569	
					0.38	0.758	
					0.47	0.947	
					0.57	1.000	
					0.66	1.000	
					0.76	1.000	
					0.85	1.000	
					0.95	1.000	
250	350	100	3	0	0.09	0.190	0.000
					0.19	0.379	0.000
					0.28	0.569	0.000
					0.38	0.758	0.000
					0.47	0.948	0.000
					0.57	1.000	0.007
					0.66	1.000	0.018
					0.76	1.000	0.027
					0.85	1.000	0.036
					0.95	1.000	0.044
250	700	100	3	0	0.09	0.190	0.000
					0.19	0.379	0.000
					0.28	0.569	0.000
					0.38	0.759	0.000
					0.47	0.948	0.000
					0.57	1.000	0.007
					0.66	1.000	0.016
					0.76	1.000	0.025
					0.85	1.000	0.034
					0.95	1.000	0.042
0	350	100	1.65	0	0.07		0.000
					0.14		0.000
					0.20		0.000
					0.27		0.000
					0.34		0.000
					0.41		0.000
					0.47		0.000
					0.54		0.000
					0.61		0.000
					0.68		0.000

Table A.2: Results of REquil-model simulations.

NO	SO$_2$	T	$t_{reaction}$	Water content	ClO$_2$/NO	NO conversion	SO$_2$ reduction
ppm	ppm	°C	s	vol.%	-	-	-
250	350	100	-	0	0.09	0.000	0.135
					0.19	0.000	0.271
					0.28	0.000	0.406
					0.38	0.000	0.542
					0.47	0.000	0.677
					0.57	0.000	0.812
					0.66	0.000	0.948
					0.76	0.117	1.000
					0.85	0.306	1.000
					0.95	0.496	1.000
250	0	100	-	0	0.09	0.190	
					0.19	0.379	
					0.28	0.569	
					0.38	0.758	
					0.47	0.948	
					0.57	1.000	
					0.66	1.000	
					0.76	1.000	
					0.85	1.000	
					0.95	1.000	
250	700	100	-	0	0.09	0.000	0.068
					0.19	0.000	0.135
					0.28	0.000	0.203
					0.38	0.000	0.271
					0.47	0.000	0.339
					0.57	0.000	0.406
					0.66	0.000	0.474
					0.76	0.000	0.542
					0.85	0.000	0.610
					0.95	0.000	0.677
0	350	100	-	0	0.07		0.000
					0.14		0.000
					0.20		0.000
					0.27		0.000
					0.34		0.000
					0.41		0.000
					0.47		0.000
					0.54		0.000
					0.61		0.000
					0.68		0.000

B

System results

Below the resulting graphs of the new NO_x and SO_x removal concept are illustrated. Two different scrubbing solutions and set ups were tested. Figures B.1 to B.4 represent the results for pure water as a scrubbing solution. Whereas the first two figures represent the vapor and liquid phase after the reactor by reaching the emission limits and the following two the results for vapor and liquid phase after the reactor for a L/G ratio of 0.5.

Figures B.5 to B.8 illustrates the results for the Water, NaOH and HNO_2 solution mix. Here the first two represent as well the vapor and liquid phase after the reactor by reaching the emission limits and the following two the results for vapor and liquid phase after the reactor for a L/G ratio of 0.5.
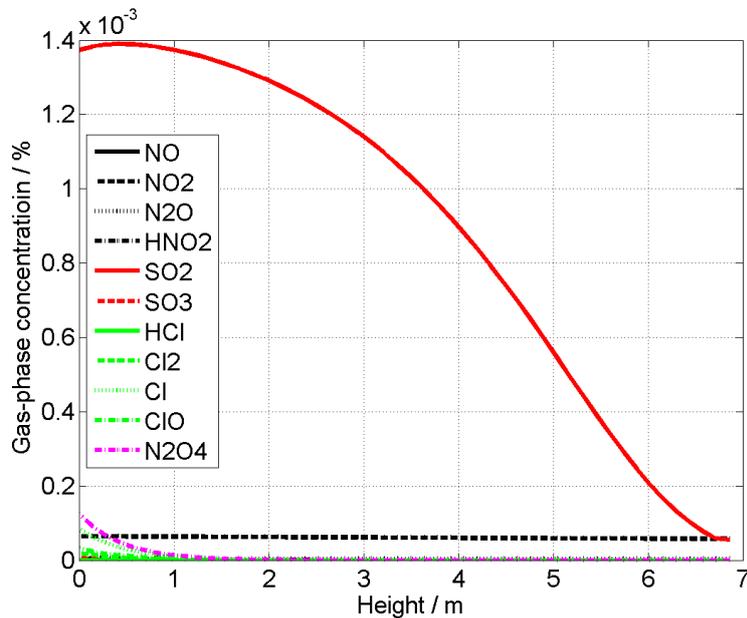
Figure B.1: Vapor composition of coal plant flue gas absorption with water amount to reach emission limits.
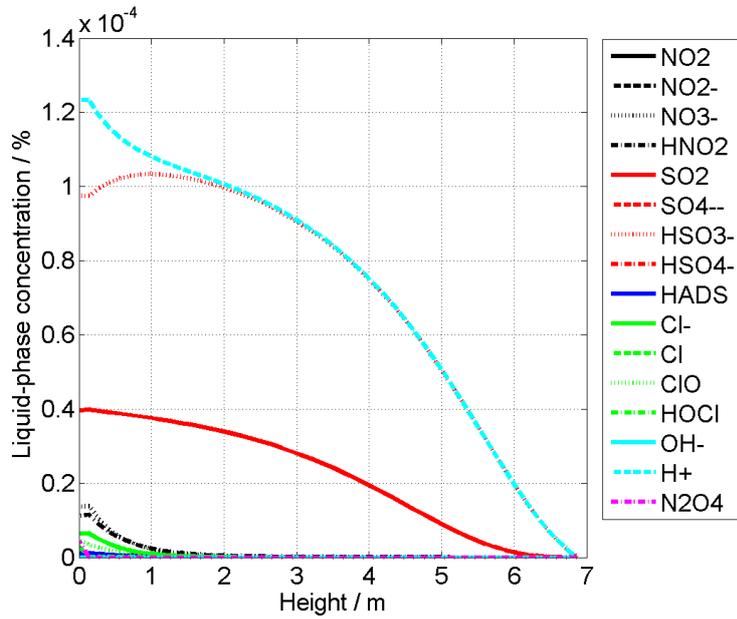
Figure B.2: Liquid composition of coal plant flue gas absorption with water amount to reach emission limits.
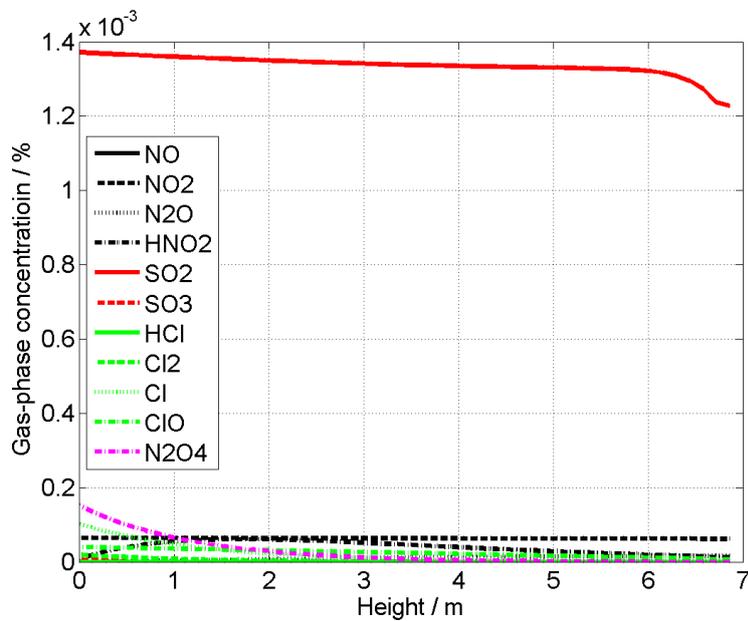
Figure B.3: Vapor composition of coal plant flue gas absorption with realistic water amount.
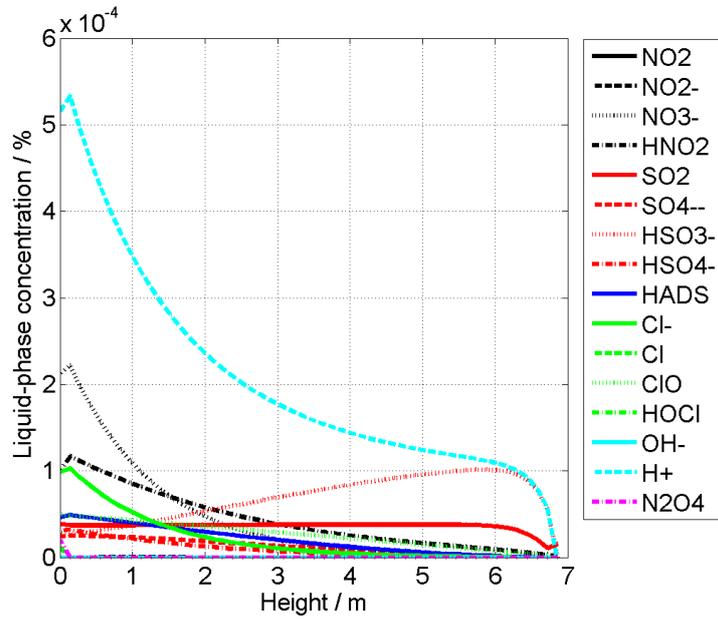
Figure B.4: Liquid composition of coal plant flue gas absorption with realistic water amount.
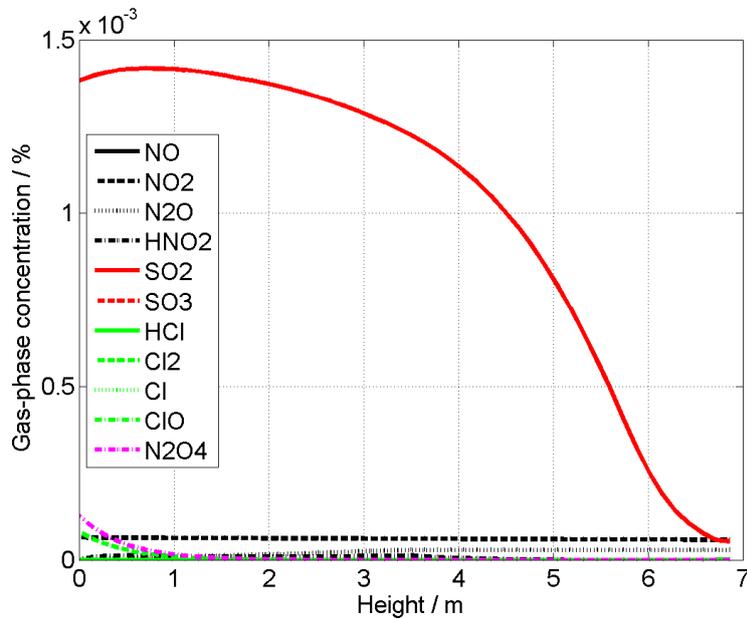
Figure B.5: Vapor composition of coal plant flue gas absorption with water amount to reach emission limits and HNO_2 and NaOH in the absorber water.
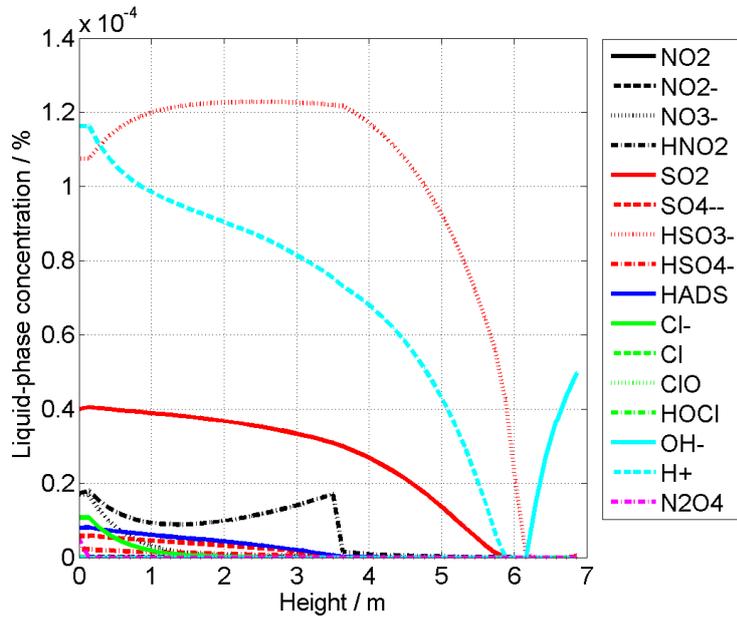
Figure B.6: Liquid composition of coal plant flue gas absorption with water amount to reach emission limits and HNO_2 and NaOH in the absorber water.
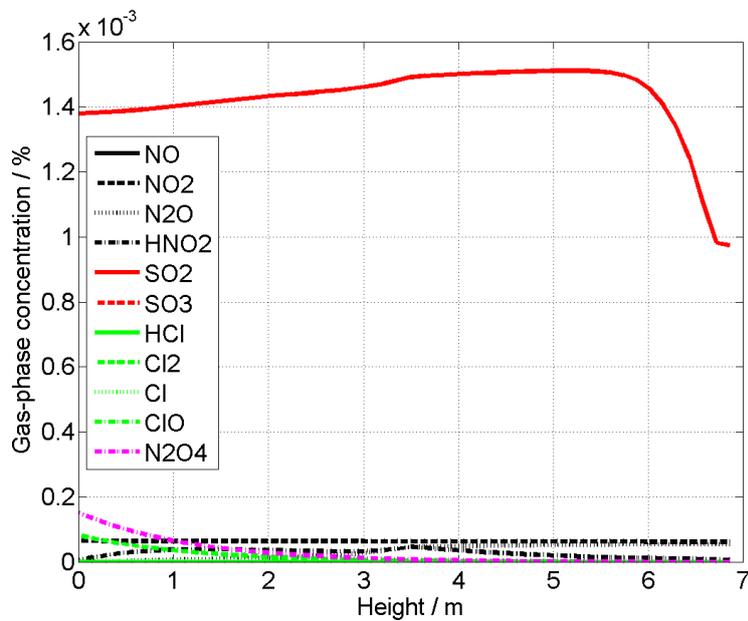
Figure B.7: Vapor composition of coal plant flue gas absorption with realistic water amount and HNO_2 and NaOH in the absorber water.
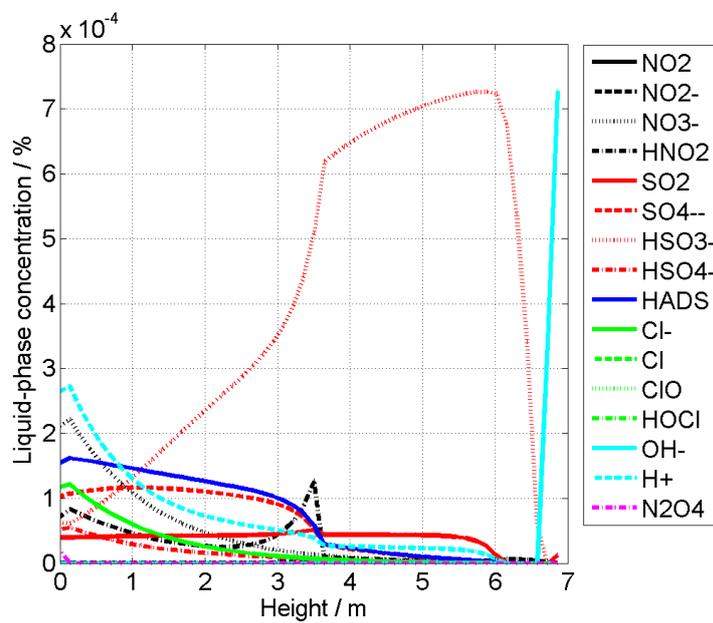
Figure B.8: Liquid composition of coal plant flue gas absorption with realistic water amount.